AD-774 567

HERTIZMAN GENERATOR DEVELOPMENT

S. D. Houston, et al

Braddock, Dunn and McDonald, Incorporated

Prepared for:

Rome Air Development Center

December 1973

DISTRIBUTED BY:

NTIS

National Technical Information Service
U. S DEPARTMENT OF COMMERCE
5285 Port Royal Road, Springfield Va. 22151

UNCLASSIFIED

SECURITY CLASSIFICATION OF THIS PAGE (When Data Entered)

AD 774 567

REPORT DOCUMENTATION PAGE		READ INSTRUCTIONS BEFORE COMPLETING FORM
1. REPORT NUMBER RADC-TR-73-325	2. GOVT ACCESSION NO.	3. RECIPIENT'S CATALOG NUMBER
4. TITLE (and Subtitle) HERTZIAN GENERATOR DEVELOPMENT		5. TYPE OF REPORT & PERIOD COVERED Final Report 6. PERFORMING ORG. REPORT NUMBER BDM/A90
7. AUTHOR(s) S.D. Houston David Bailey		8. CONTRACT OR GRANT NUMBER(s) F30602-72-C-0388
9. PERFORMING ORGANIZATION NAME AND ADDRESS Braddock, Dunn and McDonald, Inc., 5301 Central Avenue, NE, Albuquerque, New Mexico 87108		10. PROGRAM ELEMENT, PROJECT, TASK AREA & WORK UNIT NUMBERS Job Order No. 55730377
11. CONTROLLING OFFICE NAME AND ADDRESS Rome Air Development Center (OCTP) Griffiss Air Force Base, New York 13441		12. REPORT DATE December 1973 13. NUMBER OF PAGES 66
14. MONITORING AGENCY NAME & ADDRESS(if different from Controlling Office) Same		15. SECURITY CLASS. (of this report) Unclassified 15a. DECLASSIFICATION/DOWNGRADING SCHEDULE N/A

16. DISTRIBUTION STATEMENT (of this Report)

Approved for public release; distribution unlimited.

17. DISTRIBUTION STATEMENT (of the abstract entered in Block 20, if different from Report)

Same

18. SUPPLEMENTARY NOTES

None

19. KEY WORDS (Continue on reverse side if necessary and identify by block number)

Microwave
Electrical Power Conversion Devices
Generation
Wave Propagation

Reproduced by
NATIONAL TECHNICAL
INFORMATION SERVICE
U S Department of Commerce
Springfield VA 22151

20. ABSTRACT (Continue on reverse side if necessary and identify by block number)

This report summarizes the results of a one-year theoretical and experimental study of the frozen wave Hertzian concept for electromagnetic wave generation. As expected, the bulk of the effort was devoted to the switch problem, in particular switch synchronization. Several configurations are evaluated and the design of a 200 MHz generator is treated in some detail. Limitations on frequency, efficiency, power, etc., are discussed in terms of available switch technology, materials, etc.

DD FORM 1 JAN 73 1473 EDITION OF 1 NOV 65 IS OBSOLETE

UNCLASSIFIED

SECURITY CLASSIFICATION OF THIS PAGE (When Data Entered)

HERTZIAN GENERATOR DEVELOPMENT

S. D. Houston
David Bailey

Braddock, Dunn and McDonald, Inc.

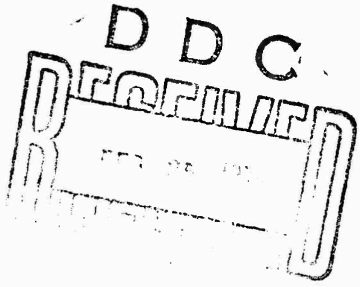

Approved for public release;
distribution unlimited.

FOREWORD

This document is the Final Report for a development effort to determine the feasibility of the Frozen Wave Hertzian Generator concept. The work was performed by Braddock, Dunn and McDonald, Incorporated, Albuquerque, New Mexico, under Contract F30602-72-C-0388, Job Order Number 55730377, for Rome Air Development Center, Griffiss Air Force Base, New York. Mr. William C. Quinn (OCTP) was the RADC Project Engineer.

This report has been reviewed by the RADC Information Office (OI) and is releasable to the National Technical Information Office (NTIS).

This technical report has been reviewed and is approved.

APPROVED: William C. Quinn

WILLIAM C. QUINN
Project Engineer

APPROVED: William T. Pope

WILLIAM T. POPE
Assistant Chief
Surveillance & Control Division

FOR THE COMMANDER: Carlo P. Crocetti

CARLO P. CROCETTI
Chief, Plans Office

ABSTRACT

This report summarizes the results of a one-year theoretical and experimental study of the frozen wave Hertzian concept for electromagnetic wave generation. As expected, the bulk of the effort was devoted to the switch problem, in particular, switch synchronization. Several configurations are evaluated and the design of a 200 MHz generator is treated in some detail. Limitations on frequency, efficiency, power, etc., are discussed in terms of available switch technology, materials, etc.

EVALUATION

Hertzian transmitters in general show promise for simple, reliable, low cost, high power, microwave generation devices at very short pulse durations eg. ten r.f. cycles. In addition, the frozen wave principle offers the opportunity for very high conversion efficiency, perhaps 60% or better.

While the frozen wave concept is simple and straightforward in principle, successful operation at a given frequency requires simultaneous closing of several switches within a time span small compared to one r.f. period. It follows that exploitation of the frozen wave principle in the microwave region will depend upon how well this criteria can be met at increasingly higher frequencies. The present study was concerned almost exclusively with u.v. synchronized overvolted spark gaps as the switch element. While no precise upper frequency limit can be stated, this study has shown that acceptable operation can be expected up to approximately 500 MHz with this switching technique. At one gigahertz and above, the need for a substantially better synchronization technique is clearly indicated.

This effort is part of RADC Technology Plan TP015.

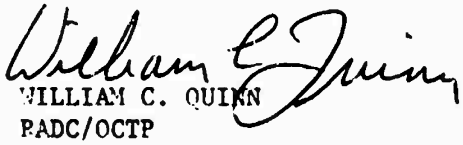

WILLIAM C. QUINN
RADC/OCTP

TABLE OF CONTENTS

LIST OF ILLUSTRATIONS

GLOSSARY

In order to simplify the discussion the following list of abbreviations and definitions is given. The system of units used will be MKS except for field strength which will be given in Volts/cm and gas pressure which will be given in either mmHg or psi on some graphs.

FWG - Frozen Wave Generator, a device that stores electric energy internally on some mechanical distribution such that the energy can be switched as a pulse train into some external load.

PCC - Pulsed Charging Circuitry, a device that can be used to charge the above to the desired energy level in a rapid and controlled manner.

UVIG - Ultra Violet Illuminating Gap, an air gap used as a source of UV energy to trigger the operation of other spark gaps.

τ_d - Statistical delay time, the elapsed time between the application of a voltage across a gap and the formation of a small ionizing current through the gap. Usually given as time after static breakdown voltage has been reached.

τ_f - Formative risetime, the time taken from the beginning of the ionization process within a gap until a current limited by the local Zo and applied voltage of the energy storage device is achieved. There are several mechanisms in operation during this process and the time may be further subdivided.

V_b - Breakdown Voltage, the voltage at which electric breakdown will occur in some reasonably long time (i.e., for dc conditions). This figure is a function of gap geometry, insulating gas pressure, electrode condition, etc., and is best used for comparison of one variable at a time.

SECTION 1

INTRODUCTION AND CONCLUSIONS

A program was undertaken to determine the feasibility of developing a high peak power pulse train generator with high effective operating frequency. The method to be examined was to be a "frozen wave" energy storage system combined with a spark gap switching scheme.

This report details the sequence and results of the program and also contains design details of a realizable 200 to 400 MHz generator with approximately 10^7 watts peak output power.

A combination of experimental and mathematical model studies was employed to characterize the microwave frozen wave Hertzian generator.

In brief it was found that switch jitter and synchronization must be on the order of 25 percent of the design period or less for effective output. At 1 GHz, the requirement is nominally 250 picoseconds.

This degree of multigap synchronization for charge voltages in the tens of kilovolts appears to be just within the state-of-the-art. It requires considerable equipment sophistication to realize.

Achieving 5 to 10 GHz operation in excess of 10^6 watts using the frozen E-wave principal, would require a considerable advancement of the state-of-the-art, particularly to realize a transportable unit.

For multicycle output at high power levels, effective gap resistance becomes an issue. Better characterization of discharge and ionization processes is required. This is especially so in the subnanosecond regime.

The major conclusions of the program are:

(1) Frozen wave generators are practical devices within the limits of current engineering practice if one restricts the peak power levels to 10^7 to 10^8 watts and the upper frequency limit to around 500 MHz or less. At this time overall system efficiencies are not especially good, on the order of 10 percent.

(2) Operation of frozen E-wave gererators at or above 1 GHz is a much more challenging task that will require quite detailed understandings of discharge and ionization processes at times well below a nanosecond. This advance will probably need a consistent and well planned long range research program. Such a program would require close monitoring of the literature and a theoretical and experimental supplement.

SECTION II

DESIGN GOALS

The initial objective of this program was to examine the feasibility of using spark gap generators to provide pulse trains with some combination of high peak output power, high effective frequency content, high overall system efficiency, and simplicity of overall design.

The proposed general configuration was to be some mechanically periodic structure that would be charged relatively slowly to some high electrostatic potential until such time as spark gaps were triggered allowing the release of this energy as a pulse train.

It was desired to attempt a breadboard model with the following parameters:

1)	Effective Output Frequency	1.3 GHz
2)	Pulse Duration and Envelope Shape	10 RF cycles, Rectangular
3)	Peak Output Power	3×10^6 watts
4)	Pulse Repetition Frequency	400 pps.

The development of a scheme that could be scaled upward or improved in all parameters was considered highly desirable. In particular, at this frequency, peak powers of about 10^8 watts and a p.r.f. of 1 kHz with 50 percent overall efficiency was specified.

SECTION III

PROGRAM OUTLINE

After a general study of the literature available (see references, Section VI) at the time the following general program approach was selected:

(1) The first stage was to be actual verification that spark gap switch operation could be achieved at a fast enough closure time to be useful.

(2) A preliminary design concept was to be selected and fabricated. The resulting hardware would then be tested and that data used in design and development of improved versions.

(3) A final design version would then be reached that would meet the design goals, or as nearly so as possible, within the constraints of the present project.

The first portion was essentially a duplication of the work by Nesterikhin, et. al., (12) and was prompted by a review of both this work and the efforts of Fletcher, et. al. (7). The reason behind this step was to gain confidence in both the authors' conclusions and to verify the operational suitability of our instrumentation.

The second portion was given a more detailed plan and organization but since it depended heavily on experimental results, it is not surprising that frequent modifications of this effort were necessary. It is this portion of the total effort that is given the bulk of the attention in the section entitled RESULTING EFFORT AND DATA.

The third portion was only partially successful. After consideration of the results of the experimental effort, it was decided that the present

achievement of a 1.3 GHz pulse train generator was rather optimistic. The reason for this was contained in the difficulty of achieving synchronized multiple spark gap operation with total jitter and risetime tolerances of around 100 psec. The design for a 200 MHz pulse train generator, given later in this report, is a more realistic and still usable end result for the present effort. To go from a laboratory demonstration to a functional system requires greater mechanical sophistication.

SECTION IV

RESULTING EFFORT AND DATA

1. FAST GAP CHARACTERIZATION

The work of Nesterikhin (12), et. al., suggests the possibility of achieving triggered spark gap closure times in the subnanosecond range with the possibility of closures in a very few picoseconds definitely worth investigating. Their system was essentially duplicated, Figure 1, and after some effort we were able to verify the feasibility of triggered spark-gap operation with jitter and risetimes at least as fast as our instrumentation (≈330 psec). These data are given in Table 1 and Figure 2. The principal result was that such risetimes could be obtained, and that a measurable population of the pulses had formative delay times of less than this amount.

2. INITIAL GENERATOR CONFIGURATION (750 MHz)

a. Key Parameters

The key operating parameters of the initially selected generator configuration are as follows:

- Nominal operating frequency — 750 MHz
- Number of chargeline segments — 4
- Number of spark gaps — 5
- Nominal Peak operating voltage — 12.5 kV
- Number of pulses per pulse train — 4 cycles
- Nominal Output energy per pulse train — 15 mJ
- Nominal Peak output power — 3 MW

A schematic and mechanical layout of the generator configuration is indicated in Figures 3 through 5.

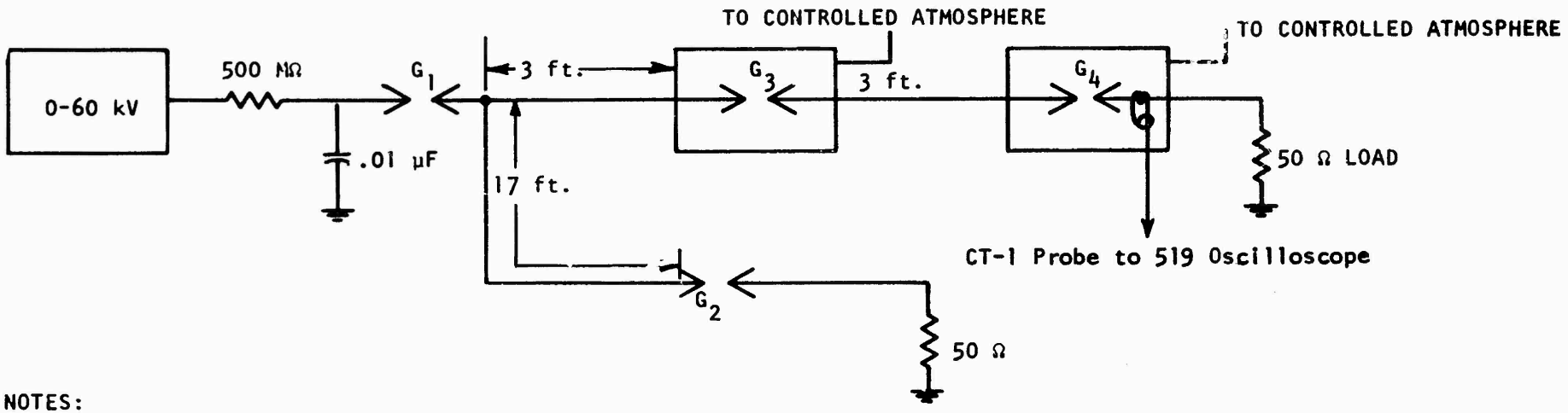

NOTES:

G_1 - G_4 ADJUSTABLE GAPS

G_1 - SPHERICAL

G_2 - G_4 - 20 mm DIAMETER PLANAR

G_3 - TRIGGERED BY UV FROM G_2

50 Ω COAXIAL CABLE BETWEEN GAPS

Figure 1. Subnanosecond Gap Test Arrangement

TABLE 1

LAG TIME SCATTER

TEST CONDITION	TIME IN NANOSECONDS						TOTAL SHOTS
	0-1	1-2	2-3	3-4	4-5	5-6	
No Illumination	.8	1.2	2.3			5	11
	.9	1.6				5.1	
		1.9				5	
		1.8					
		1.6					
Illuminated (6 inches)	.8	1.1	2.7		4.6		24
	.3	1.9	2.4				
	.6	1.8	2.8				
	.6	1.9					
	.9						
	.6						
	.6						
	.7						
	.9						
	.9						
	.7						
	.4						
	.4						
	.8						
	.6						

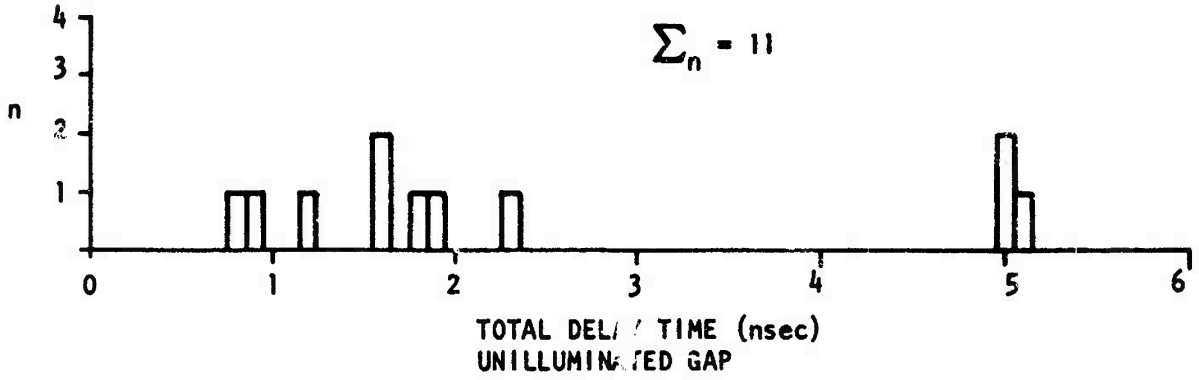

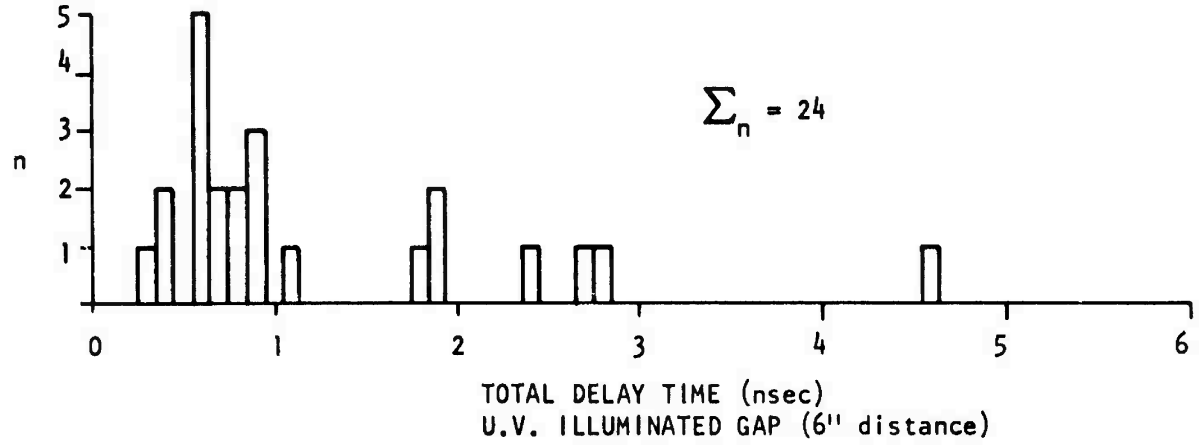

Figure 2. Histogram of Lag Time Scatter Data

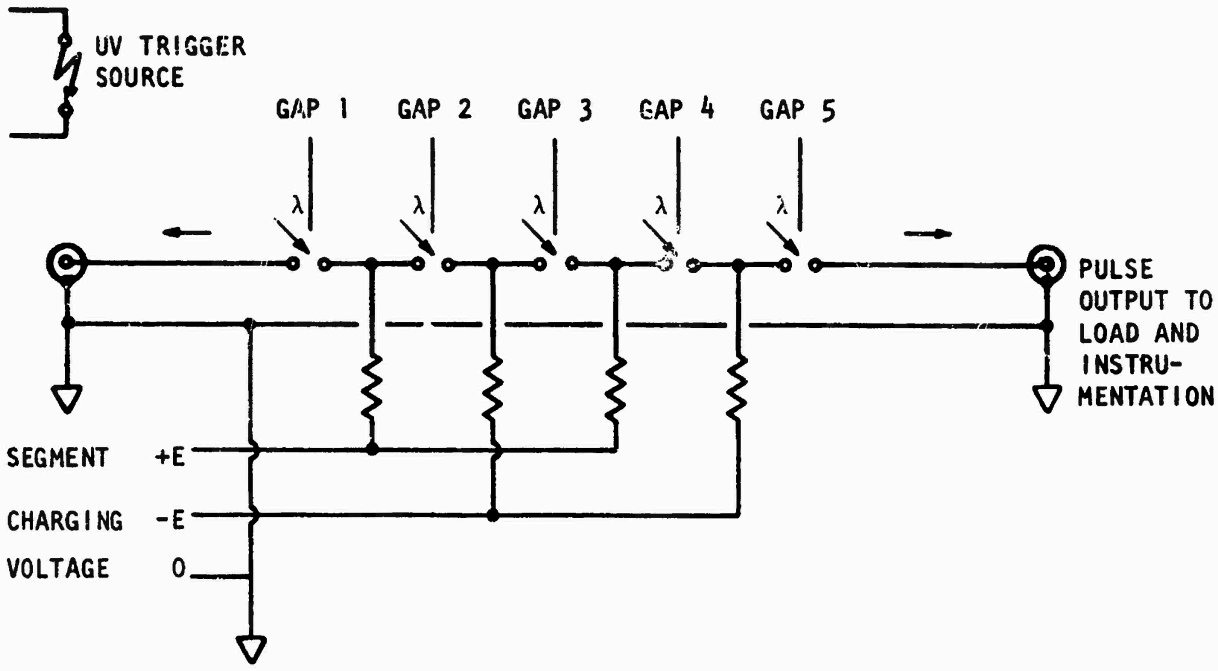

a. Functional Schematic Charged Line Section, 750 MHz Generator

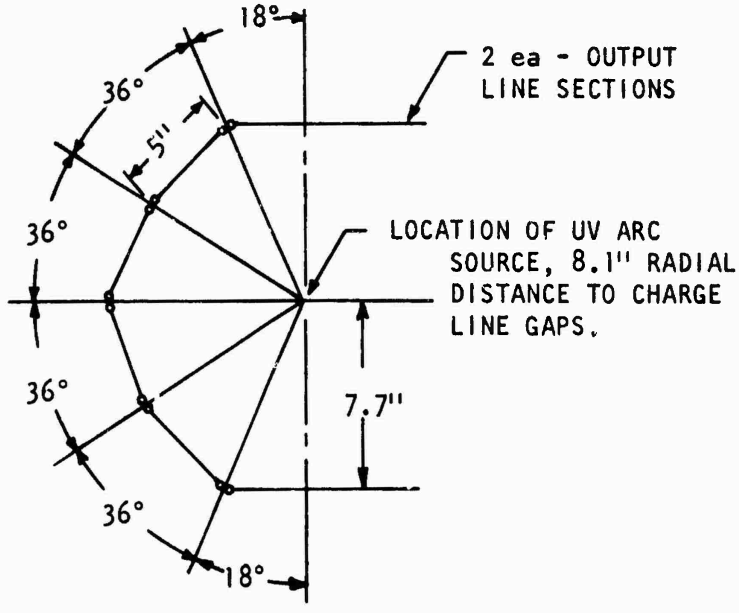

SCHEMATIC PLAN VIEW

b. Positional Layout for Spark Gaps, 750 MHz Generator

Figure 3. 750 MHz Generator

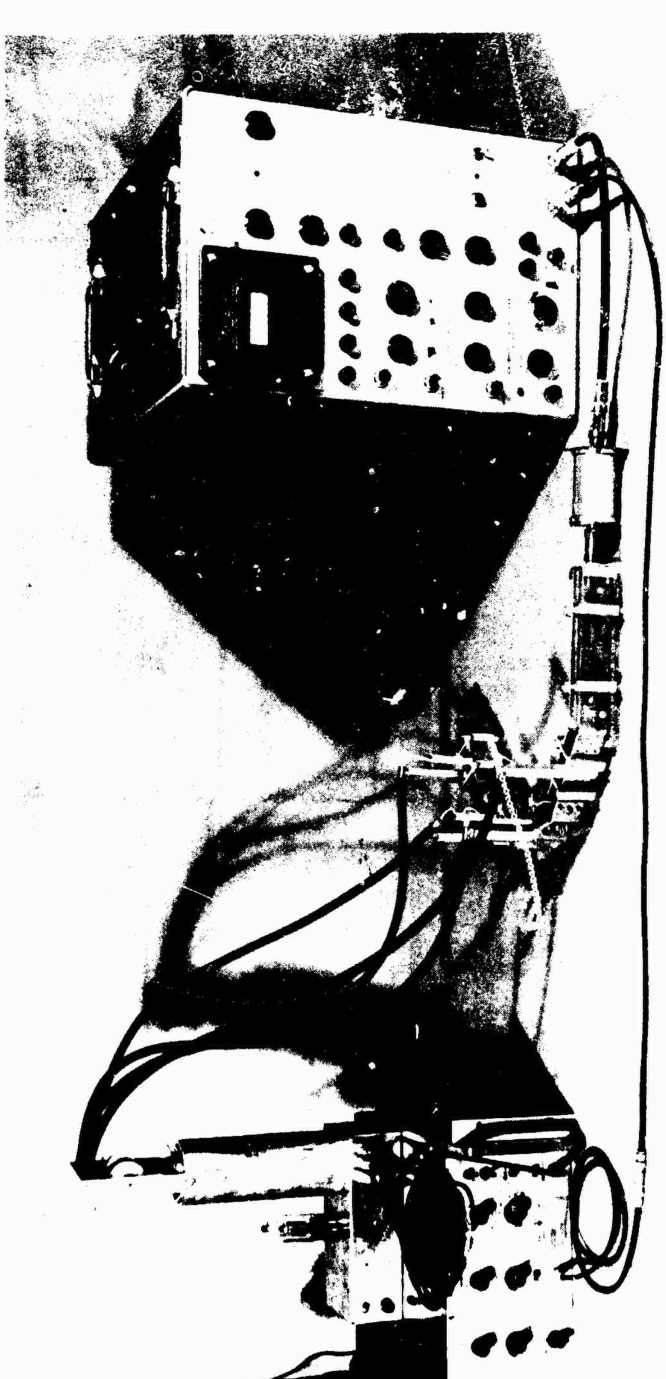

Figure 4. Hertzian Generator Assembly and Associated Apparatus

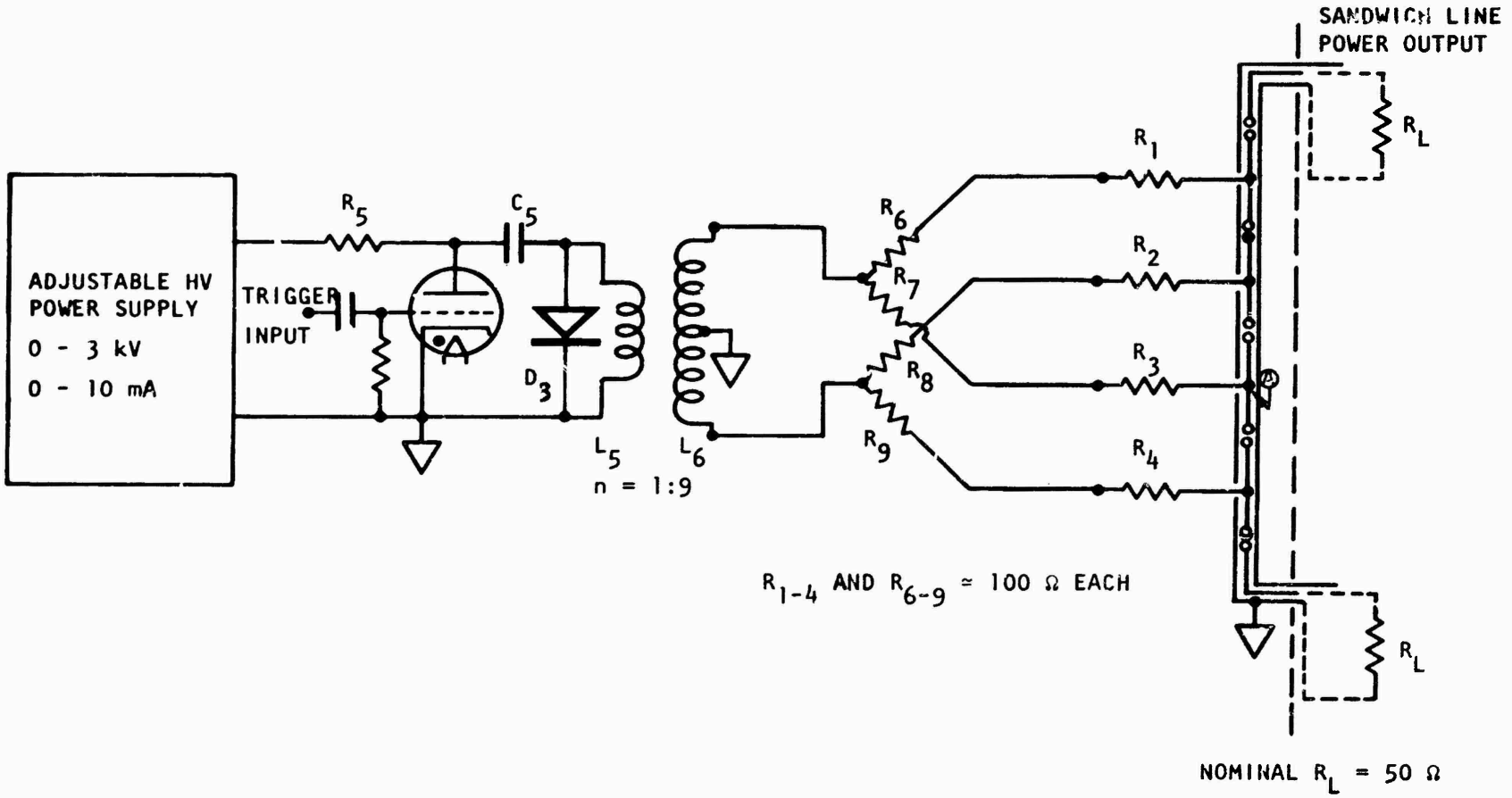

Figure 5. Pulsed Charging Circuitry

The "horse shoe" shaped geometry was selected to locate the segmented line gaps on the circumference of a circle; the purpose being to have the UV triggering illumination arrive at all gaps simultaneously. The illuminating air arc was not intense enough to get the desired operation, however, the principle seems well justified and deserves further investigation. This point is discussed later.

b. Problems Encountered

In the course of operation attempts a few very important details were encountered. They included the requirement for 1) adequate decoupling between the generator and the pulsed charging circuitry when the generator was operating, and 2) matching the PCC driving impedance to that of the load presented by the many line segments in parallel before the generator began its operating cycle. These are somewhat conflicting requirements for which no really satisfactory solution was obtained. The best apparent solution is to charge the line segments with as high a voltage as practicable in as little time as possible. This allows one to use a small but reasonably useful series isolation resistance between the various line segments. Ideally one wants the series impedance of this isolation element to be low for the charging voltage and still be high for the generator output pulse train. Because the charging time is at least on the order of the output pulse train duration reactive components are not very useful for this function. A lossy, brute force resistive device is an unelegant but acceptable solution.

If very many segments are to be charged in parallel, the charging circuitry switch must have some performance characteristics as good as, or better than the segment gap switches used. This could be a rather stringent requirement. For illustration of this point suppose that one wished to change 10 line segments to 25 kV in 150 nsec. If each line segment had 50Ω characteristic impedance and was charged at its midpoint this is an initial effective load of around 2-1/2Ω.

This suggests a total peak charge current of about 10K amps. If each line segment had a total capacitance of 50 pF and was driven by 2-1/2Ω charging resistance this gives 1 time constant of 1-1/4 nsec but a 2-1/2Ω driving impedance is not very practicable from an engineering end-point.

Another requirement mentioned was encountered in the operation of the UV Illuminating Gap (trigger source). About 10-16 times the intensity available appeared to be needed to achieve reliable simultaneous gap triggering under the E/P conditions used. This was determined by monitoring the operation of a single gap as the UVIG was moved closer from its nominal central position. At a gap-gap distance of less than 3 inches fairly reliable triggering was obtained, whereas at the nominal distance of about 8 inches operation was rather erratic. The stored energy at the time of the UV illuminating gap breakdown was estimated to be 15 mJ (5 ft of RG/8 charged to 14 kV) of which about 2 percent or .3 mJ (1Ω arc resistance driven by 50Ω line) was deposited in the arc proper.

The overall FWG operation was seriously degraded by jitter contributed from several sources. Improving the risetime of the voltage driving the UVIG could reduce this total jitter some but a more important improvement can be achieved by reducing the risetime of the UVIG once breakdown starts. This means that the triggering photon intensity is more nearly a step function. Since this intensity follows the current closely any scheme to lower the local driving impedance is an improvement. Here we mean local in a time sense, perhaps 10-50 psec. Lowering this impedance will also improve the energy transfer from the drive line to the arc plasma. The use of a good r.f. capacitor in the structure supporting the UV gap would accomplish this purpose.

Another improvement in UV intensity could be obtained by increasing the arc resistance for a time less than around 100 psec.

Perhaps this could be done by enclosing the arc in an open ended but narrow bore capillary tubing. This would have to be of a UV transparent material (e.g., fused silica), and the bore diameter would be about .010 mm, a rather small value. The effects of the confining wall and inertia of the air piston would maintain a higher pressure in the arc for more efficient transfer of the stored energy to the plasma.

A third area of considerable importance to the successful operation of this generator is the absolute pressure and composition of the insulating gas between the gap electrodes. The particular combination of nominal operating frequency and power output selected for this generator will not tolerate much variation in gas pressure, as evidenced by the difficulty in adjusting the gap spacing such that all gaps could be triggered simultaneously. The only solution to this problem is the total enclosure of the spark gap volume in a pressure tight container. This gas pressure sensitivity carries with it an equal sensitivity to gap spacing and requires good mechanical rigidity.

It is for this reason, in addition to the apparent need to operate at a nonatmospheric pressure, that the design effort for a 200 MHz system resulted in a mecnanically more complex package.

c. W/Cu Electrode Characterization

The electrodes used throughout this program were fabricated from a W/Cu composite, Elkonite 30W3 supplied by P R Mallory Co. This is characterized by good electrical/wear properties but the work function is not precisely known. The lack of data on electrode operation left questions leading to an effort to deduce the underlying operational difficulties. The data represented in Figures 6 and 7 were obtained. The waveshape and times are indicated in Figure 8. This is the applied voltage for a single spark gap measured at point A in Figure 5. "Breakdown" voltage was taken to be that at which greater than 90 percent of the applied pulses caused an

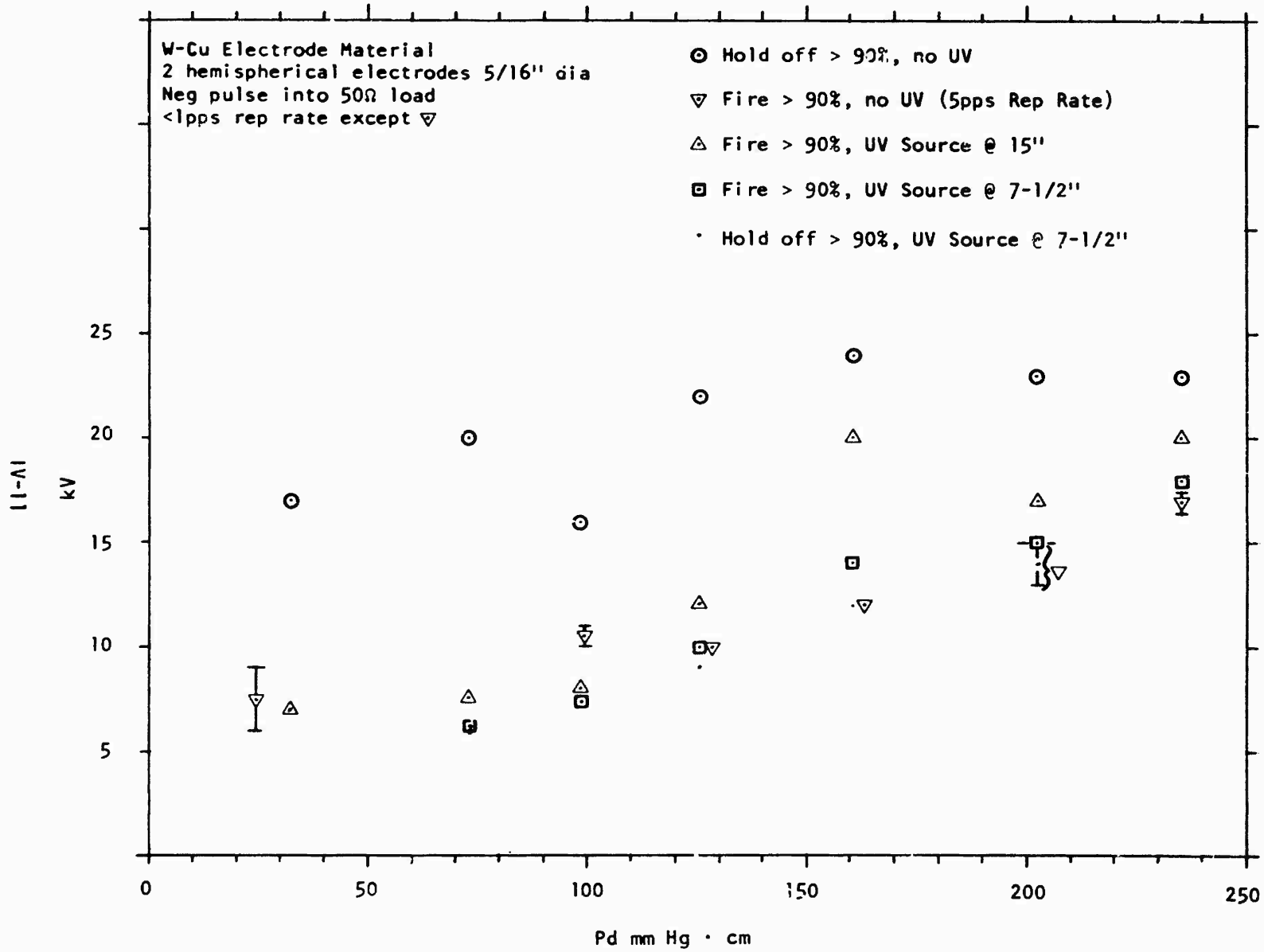

Figure 6. W-Cu Electrode Data

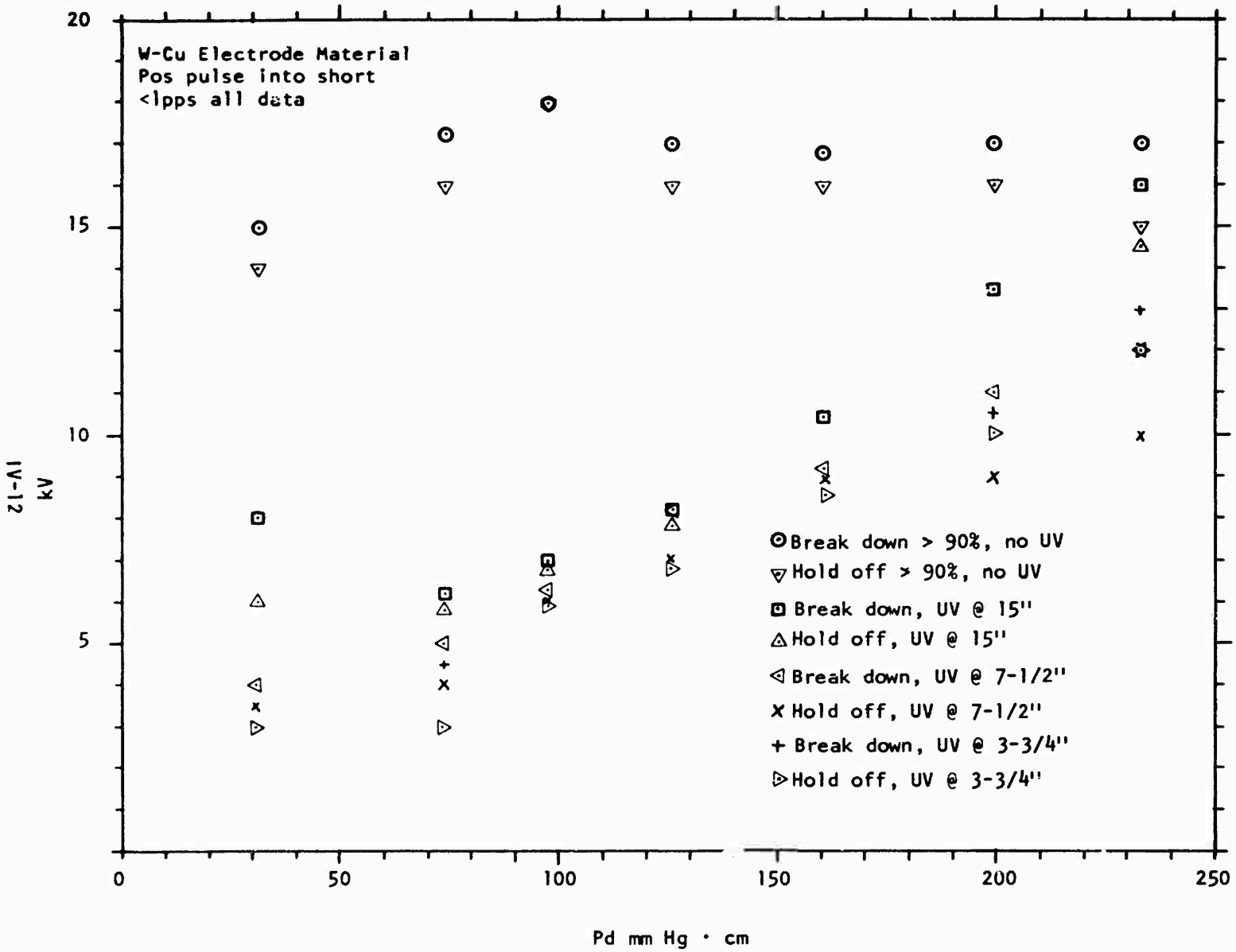

Figure 7. W-Cu Electrode Data

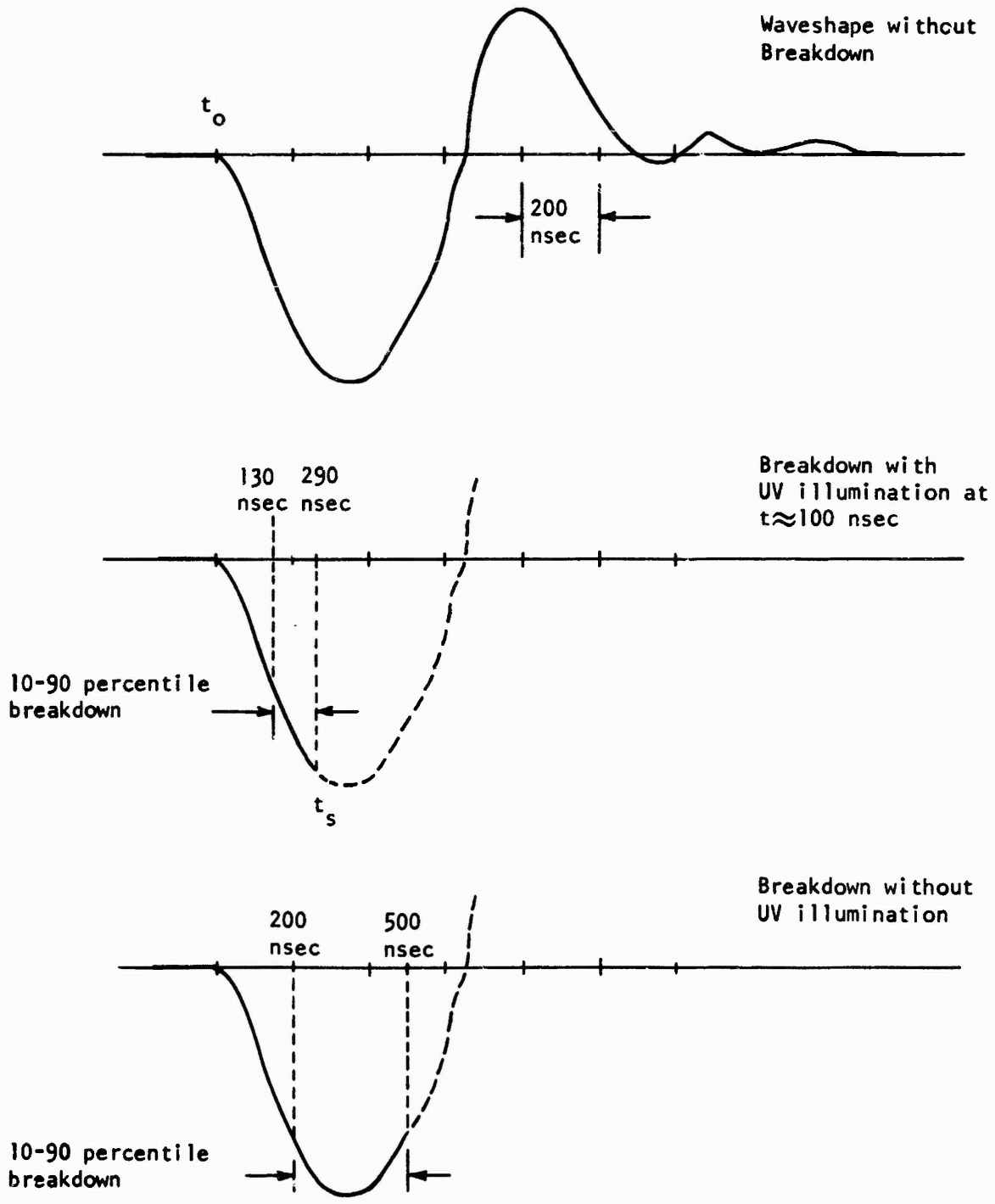

Figure 8. W/CU Electrode Data Pulse Waveshapes

arc at the electrodes during the first half cycle. In actual fact, this was not a common occurrence later than about 100 nsec past the peak voltage (e.g., at about t = 500 nsec), except for the most intense UV illumination tested. The criteria for "Holdoff" were that no more than 10 percent of the applied pulses caused an arc in the first half cycle. Breakdown during the second half cycle, at a lower peak voltage, frequently occurred but was counted as a "holdoff." The major difference between test setups for Figures 6 and 7 was the series lead impedance. For Figure 6 the load consisted of about 8 inches of 48Ω sandwich line connected to a 49-1/2Ω resistive load. For Figure 7 the load was a short circuit return. The applied polarity was reversed for the two cases (Figure 6 was negative) but because the electrodes were fairly symmetrical hemispheres and of the same material that should make little difference.

There is quite a bit of scatter in voltages obtained for the unilluminated gap. This, of course, is not unexpected, but the apparent independence of breakdown voltage on gap length is surprising. There are several uncontrolled variables including atmospheric pressure, moisture content, and temperature. Also the background ionizing radiation will be somewhat high and variable as we are generally near a granite-monzonite core mountain range and at an elevation of about 5500 feet above sea level. There is relatively little ultraviolet light in the ambient laboratory environment. It should be noted that the scatter in breakdown time is about three times larger for the unilluminated case.

The presence of UV from the open air arc lowers the holdoff voltage by an amount varying between about 30 percent for a P·d value of 235 mmHg·cm to about 75 percent for a P·d equal to 30 mmHg·cm. The resultant curve follows a Paschen's Law curve closely.

A feature that does not appear on the plots but was observed on the oscilloscope was that the holdoff time (t_s) decreased rather

uniformly from about 250 nsec for P•d values of 200--235 mmHg•cm to 150 nsec for P•d equal to 30 mmHg•cm. The jitter observed almost always was in the direction to increase t_s.

For all the data presented the UVIG breakdown jitter appeared to be the largest contributing factor, and that was on the order of 100 nsec. The delay between UV emission and test gap breakdown has not been measured but it appears that there is about 40--50 nsec delay between the beginning of current flow in the UV arc and breakdown in the test gap.

d. Rep Rate and Gap Quenching

An unfavorable situation exists, however, in that the range of control apparently exercised by the UV illuminating gap is considerably decreased at pulse rates much above 1 per second. There appears to be a residual ionization, possibly in the form of energetic ozone molecules, that lowers the breakdown voltage greatly for pulse rates above 3 per second.

At pulse rates of about 60 per second the gaps will often break down at as little as 10 percent of the single pulse voltage. UV illumination has little effect, perhaps due to the lowered holdoff potential of the gaps and due to the lowered UV arc intensity as a result of power supply limitations. Small quantities of unspecified Freon compounds mixed in with the atmosphere in the gaps increased the breakdown strength considerably but the composition was not either known, controlled, or reproducible. It was in this way easily possible to increase the gap's holdoff voltage by about twice by use of the insulating gas.

Examination of the available literature suggests several gas combinations are much better than air insofar as quenching effectiveness is concerned. Removal of oxygen from the spark gap by use of dry nitrogen has merit in its simplicity, low expense, and improved performance.

Hydrogen, carbon dioxide, the inert gases, fluorinated hydrocarbons, and sulfur hexafluoride are all potentially useful additions to speed the quenching of arcs.

e. Other Experiments

The high frequency "frozen" wave pulser, (i.e., the original apparatus used to date), was equipped with all brass electrodes. The objective was to compare the operating characteristics of the brass and W-Cu composite electrodes.

The measured pulse risetime (10-90 percent) varied from about 1.2 nsec for a .102" gap to approximately the scope limit (about 1/3 nsec) for a gap somewhat larger than .030 inches. The apparent risetime remained the same then down to a gap spacing of about .002 inches. The following figure shows the range of values found.

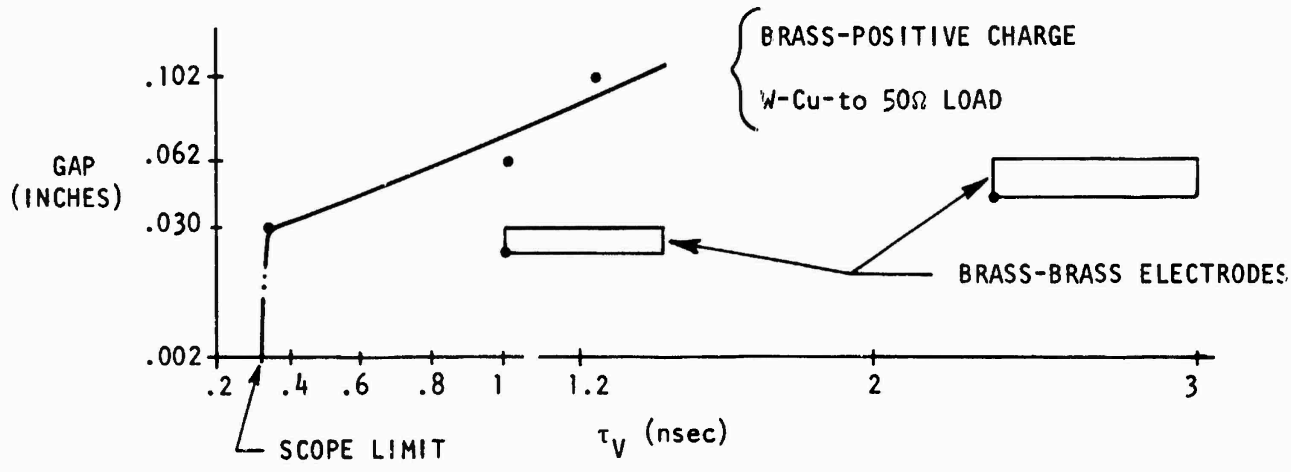

On the basis of the observation that it was difficult to achieve obvious synchronization by use of the UV illuminating gap it is thought that the brass electrodes are less sensitive to photo ionization triggering than the W/Cu electrodes.

Some jitter measurements were taken by triggering the scope sweep by the breakdown of the UV gap and recording the pulse waveshape of the measured gap. The jitter was about 3 nsec by this measurement. The delay was not measured but estimated from cable lengths and scope settings to be 15-20 nsec and was stable to about 1 nsec based on the triggering waveshape jitter.

3. LOW FREQUENCY CONFIGURATION (75 MHz)

As a result of the several experimental difficulties encountered in the original (750 MHz) configuration three serious questions were raised. The first was whether or not a frozen wave generator could be made to work above a very few MHz using ambient air for gap insulation and the second was the matter of electrode and gap characterization. The third had to do with deciding just how much tolerance existed to any jitter of spark gap operation, the results of which are treated in Section IV.4.

a. Test Method

To at least partially answer this question a low frequency version of a frozen wave generator was fabricated. The nominal frequency was to be about 70-75 MHz, well within the range of all our instrumentation. The order of magnitude change in timing requirements was expected to provide more understandable data. The mechanical arrangement is indicated in Figure 9. The charging voltage used was from two sources; one was the same unit used for the 750 MHz configuration, the second source used was two independently adjustable dc power supplies charging the line segments through several megohms

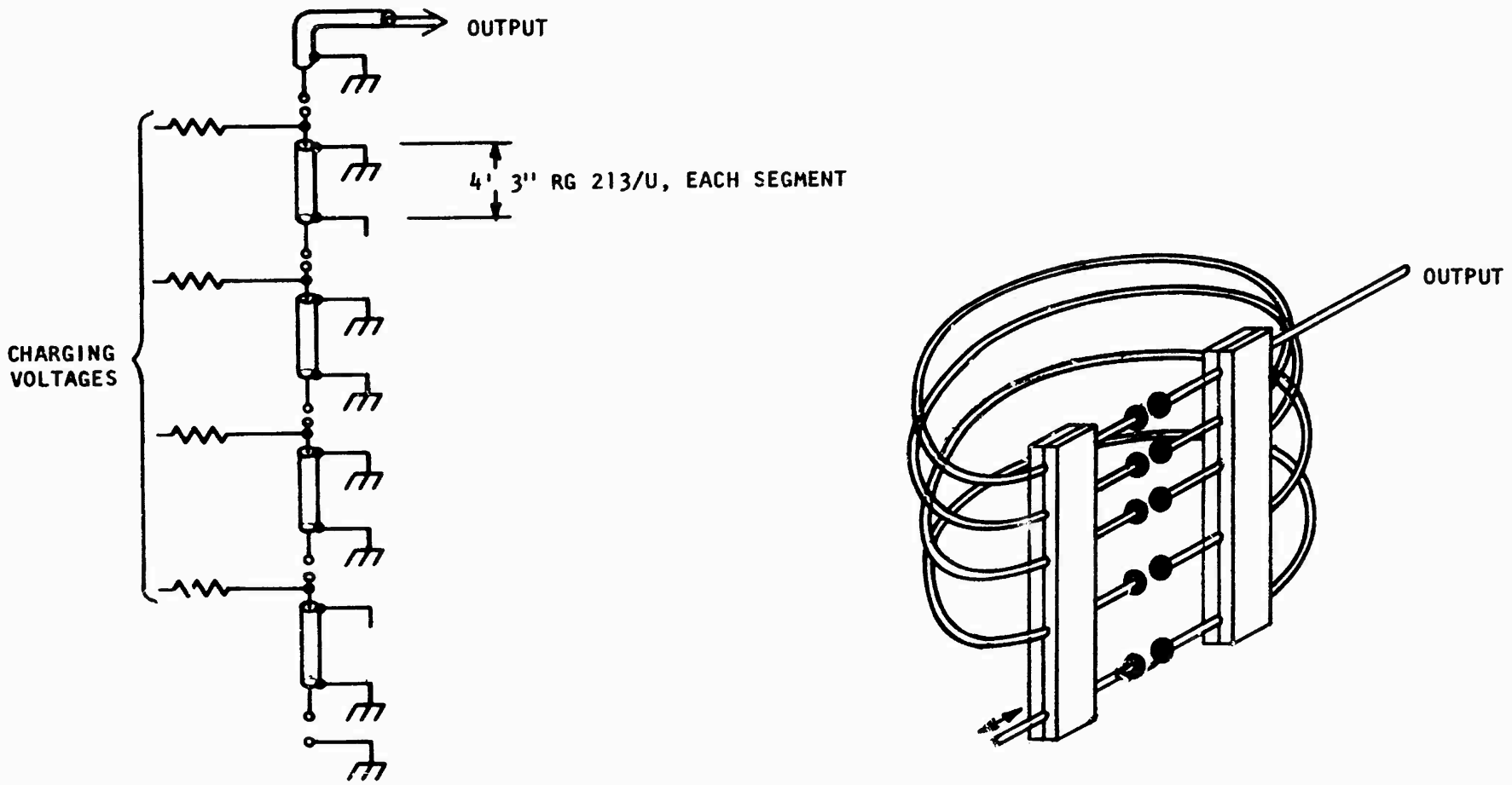

Figure 9. Mechanical Arrangement, 70 MHz System

series resistance for each segment. In this configuration several combinations of pulsed and dc segment charging were used with pulsed and dc UV illumination for triggering. The unit was basically 4 segments of RG 213, 130 cm long with 13 mm diameter brass balls for electrodes. Consecutive gaps were ≈ 30 mm apart and could "see" each other. This unit was operated in an uncontrolled atmospheric ambient in both the pulsed charging mode and the dc charging mode. By charging various combinations of segments different output waveshapes were available.

b. Frozen Wave Operation

The best operation was achieved by charging the line segments until one gap broke down and the resulting UV triggered the remaining gaps. This resulted, however, in low overvoltage factors and the waveshape was not especially good. The pulsed charging mode was not successful, apparently because the self-resonances of the pulse charging circuitry could not be separated from the operating period of the 70 MHz generator. Damping the ringing with larger series resistances reduced the available charge voltage below a usable level.

At this point the examination of several scope traces showed a few photos with approximately expected waveforms. (Figure 10) Although inconclusive it appears that the Frozen Wave Principle has been demonstrated but more mechanical improvements are needed for functional operation.

For the case where the unit was powered with the PCC the gaps used were in the range of .065 to .050 inches. The basic discovery was that two segments were the maximum usable number without extremely critical (and unstable) adjustment of the spark gaps. It was possible to obtain reasonable waveshapes including open circuit and short circuit reflections for 2 segment operation. For three segment operation one could occasionally view direct output pulse trains of reasonable

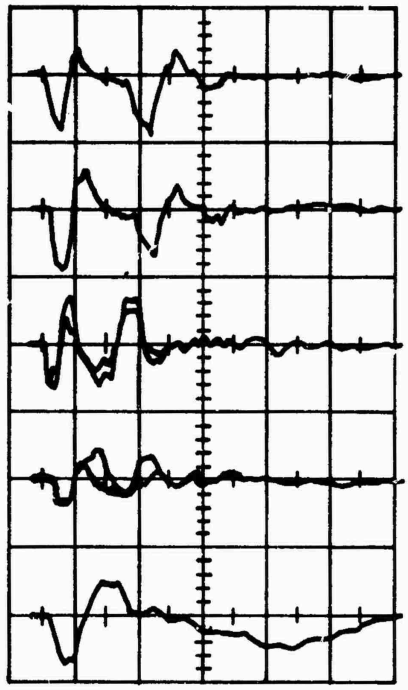

Trace #1, 2 2 segments charged opposite polarity, DC to self breakdown, reflection from open circuit at end of 2 more segments, UV triggered

Trace #3 3 segments charged, otherwise same as above

Trace #4 Same as #3, short circuit reflector

Trace #5 2 segments pulse charged, no reflecting segments on ckt.

Vertical, 3.33 kV/cm, Horizontal 20 nsec/cm

Figure 10. 70 MHz System Operational Photographs

waveshape but the reflected pulse trains were almost never coherent enough to give readable scope traces. These results could not be obtained with any regularity at all for four segment operation.

In all cases, operation was erratic with pulse train operation occurring for a few seconds at a time interspersed with considerable random appearing operation. This was thought to be due largely to variations in atmospheric pressure due to the dynamics of the building air-conditioning.

c. "Traveton" Operation

A second technique was briefly examined. In this case, one or more segments were charged with a single polarity and the resulting pulse shape was observed. This is similar to the "Traveton" technique used elsewhere. The most promising output pulse was obtained with the segment farthest from the output end charged to breakdown voltage. The resultant pulse was then allowed to break down subsequent segment gaps, at a much smaller electrode spacing, eventually reaching the output cable.

The pulse amplitude decreased with an increasing number of uncharged line segments but, to a first order approximation, the total energy under the pulse train did not decrease at a rate greater than 15 percent for each additional segment.

The pulse risetime could be improved by reducing the gap length for all gaps but this also reduced the pulse amplitude. The pulse waveshape was best for the case with two intermediate segments for first gap spacing in the range of .127 to .166 cm. The firing voltage was on the order of 2-1/2 - 3 kV for this case. By closing the gap spacing to a distance on the order of .025 cm, the best output could be reached with three intermediate segments but the pulse voltage was now about 600-1000 volts.

4. MODEL TIMING AND GAP LOSSES

Various analytical models have been examined to determine to some degree the timing and gap resistance effects upon operation. The line segments were equated to a lumped constant delay line with several sections and the response to various switch closure timings was examined by means of a computer program NET-2. This program was specifically established some years ago to study behavior of rather complex passive component circuits and networks with regard to time varying signals.

The circuit analog to an incremental segment of transmission line is sketched below.

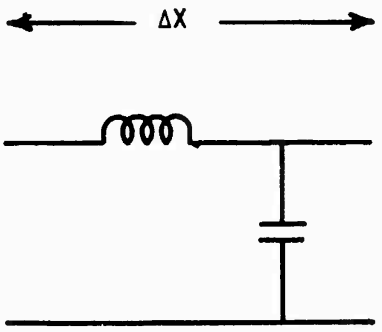

This can be used to build a discrete element representation of the microwave Hertzian generator where strip line, lecher line, or coaxial line configurations may be employed. This representation then can be used to study time dependent behavior directly.

The basic frozen wave generator which was studied in this program consisted of a four segment, five spark gap physical configuration. Each of the segments was 1/2 wavelength long at the design frequency and alternate segments were charged to equal but opposite potentials. The spark gap at one end discharged the end segment into a short circuit while the gap at the other end discharged into a resistive load matched to the line impedance. This resistive load simulates the generator output load. The intermediate gaps, when fired, complete the transmission line.

Each segment of the FWG was modeled as follows:

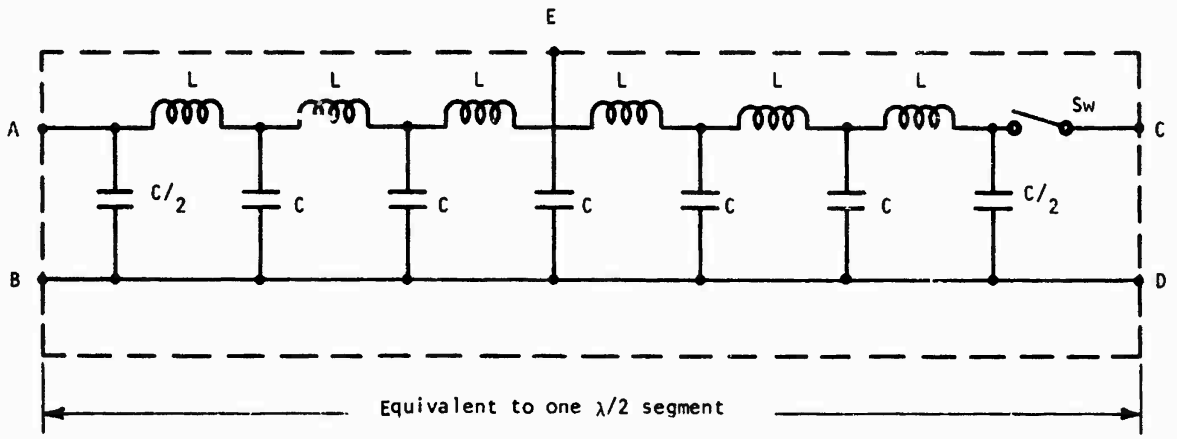

The switch represents the spark-gap and the L's and C's are derived from the line characteristic impedance and phase velocity. That is

$$Z_c = (L'/C')^{1/2} \text{ in ohms,}$$

$$\nu = (L'C')^{-1/2} \text{ in meters/second,}$$

so that

$$L' = Z_c/\nu, \text{ the inductance per unit length}$$

and

$$C' = 1/Z_c\nu, \text{ the capacitance per unit length.}$$

Then

$$L = 1/6\ L'\ \lambda/2,$$

and

$$C = 1/6\ C'\ \lambda/2\ .$$

Using the above building block the four segment FWG becomes

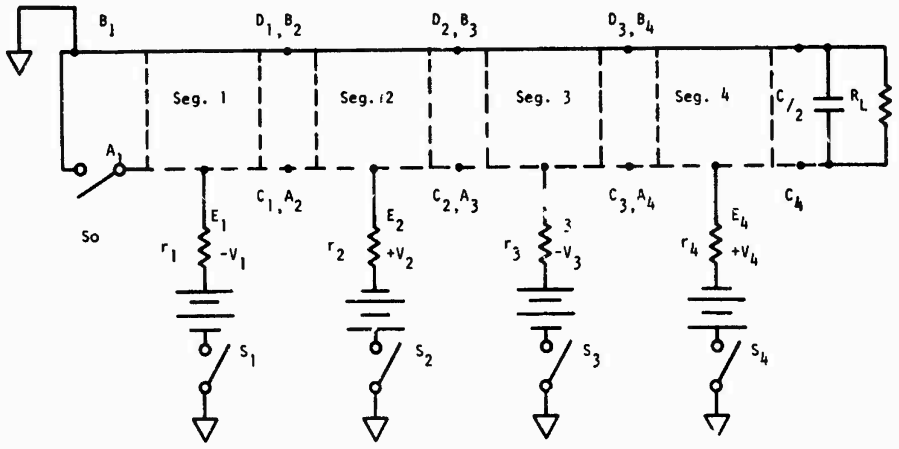

Where the combination $\{r_i, V_i, S_i\}$ is symbolic of the time dependent segment charging circuitry. It may be replaced in general with a $V_i(t)$.

a. Timing

For the timing study a design frequency of 1 GHz, a line impedance of 10Ω, and a phase velocity of 3×10^8 meters/second were selected. Then λ is 30 cm, each L is 8.33×10^{-4} microhenries and each C is 8.33 picofarads.

Switches S_1 through S_4 are closed allowing the segments to reach a steady state. This is on the order of 0.5 to 5 nanoseconds depending on the details of the charging cycle circuitry. These switches are opened and

"triggering" is initiated. That is switch S_o and the switch internal to each segment is given a time dependent command to close, completing the transmission line.

As a baseline, S_o and the segment switches are closed simultaneously. The result is a fairly uniform cyclic output for 8 half cycles at 1200 to 1300 Volts peak to peak (1000 volt segment voltage) with little harmonic distortion.

Next, a number of arbitrarily selected switch sequences were selected (i.e., 0, Seg 1, Seg 2, Seg 4, Seg 3; Seg 3, Seg 4, Seg 2, 0, Seg 1; etc.) For each sequence a closure time interval was given different values from 1/10 τ_r to 5/8 τ_r, where τ_r is 160 picoseconds, the 10 to 90 percent risetime for a sinusoid at 1 GHz. As the interval was increased there was only small spectral degradation and amplitude loss up to a 64 picosecond sequence interval. At 100 picoseconds the output is severely distorted, the principal degradation being in loss of spectral content at the design frequency.

The 100 picosecond sequence interval corresponds to a mean pair wise switch interval of 200 picoseconds with an [rms] spread of 64 picoseconds. This implies then that for useful coherent output from a frozen wave Hertzian generator, segment to segment switching must be accomplished such that the mean gap to gap (all pairs) timing is simultaneous to times shorter than 1/4 period at the design frequency.

b. Gap Losses

The above model was modified to investigate output versus waveform for an increased number of segments (1/2 cycles) when losses are considered.

In general a spark gap may be modeled as sketched below.

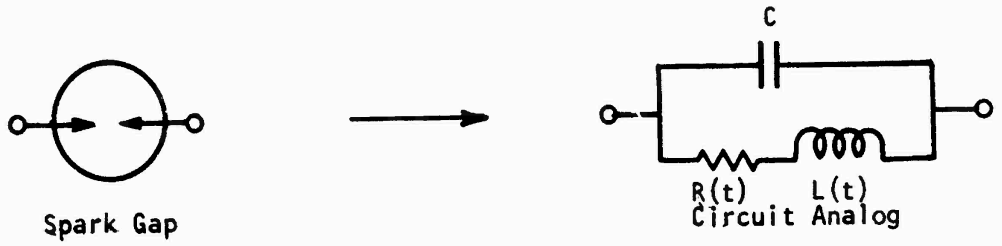

C is determined by the gap geometry. For the dimensions of experimental apparatus discussed elsewhere, the gap capacitance is on the order of 0.2 picofarad compared to a nominal 50 picofarads for each segment.

L(t) is principally a function of geometry but to some extent depends upon the dynamics of arc growth. For the geometries here, its late time value is on the order of 10^{-10} to 10^{-9} henries. R(t) is a strong function of arc dynamics and gap separation and is nonlinear. That is during arc growth the V-I characteristic could be represented by $I(t) = k(V(t))^n$ or

$$VI(t) = \left(\frac{V^{(-n+1)}}{k}\right) I(t)$$

implying an effective R (t) of the form

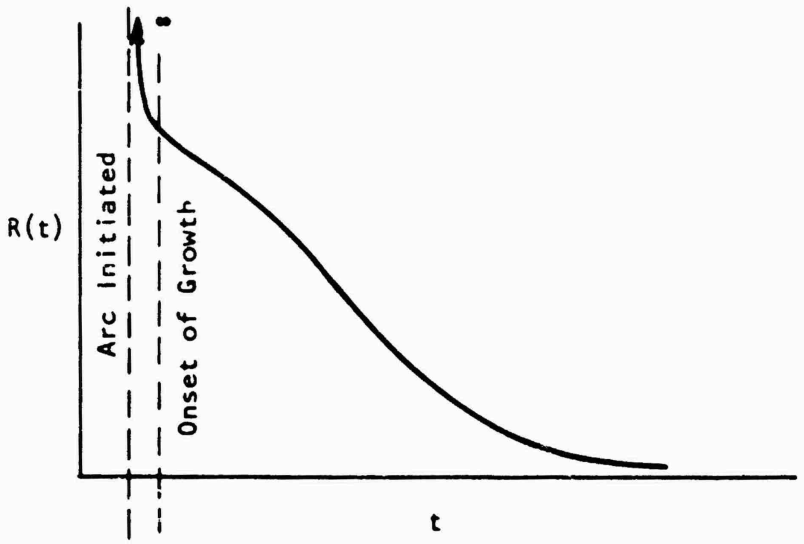

As a first approximation for estimating gap losses the R(t) was taken as a two level device switching instantly from infinite resistance to a small constant value.

A six segment, seven gap Hertzian Generator was modeled as before and effective gap resistances of 0.6Ω, 1.2Ω, and 3.0Ω considered. The first two cases show small differences as would be expected while the 3Ω case exhibits significant late time power losses. The 1.2Ω and 3.0Ω curves are shown in Figures 11 and 12 respectively.

For zero gap resistance the average power out in the example (10Ω line, 1 GHz) is 2.1×10^4 watts per (kilovolt charge)^2 or 10^7 watts for 23 kV charging voltage. At 1.2Ω per gap the average over six cycles is 1.2×10^4 watts per (kV)^2 and at 3.0Ω per gap it is 0.8×10^4 watts/(kV)^2. In the latter case nearly ninety percent of the available energy is in the first 3 cycles as opposed to 74 percent for 1.2Ω and 50 percent for zero ohms.

It appears that for per gap resistance on the order of 10 percent of the line impedance, a point of diminishing returns is rapidly approached where there is little to gain in increasing the pulse train length (number of cycles of output).

Gap losses can be minimized by increasing the line impedance and load resistance. However, realizing the highest initial peak power would then require a square root increase in charge voltage. Increasing charge voltage implies increased pressurization to maintain standoff. Greater pressurization implies decreased mean free path and uncertain increases in gap resistance. There appears to be a delicate balance involved in realizing optimum power/energy output.

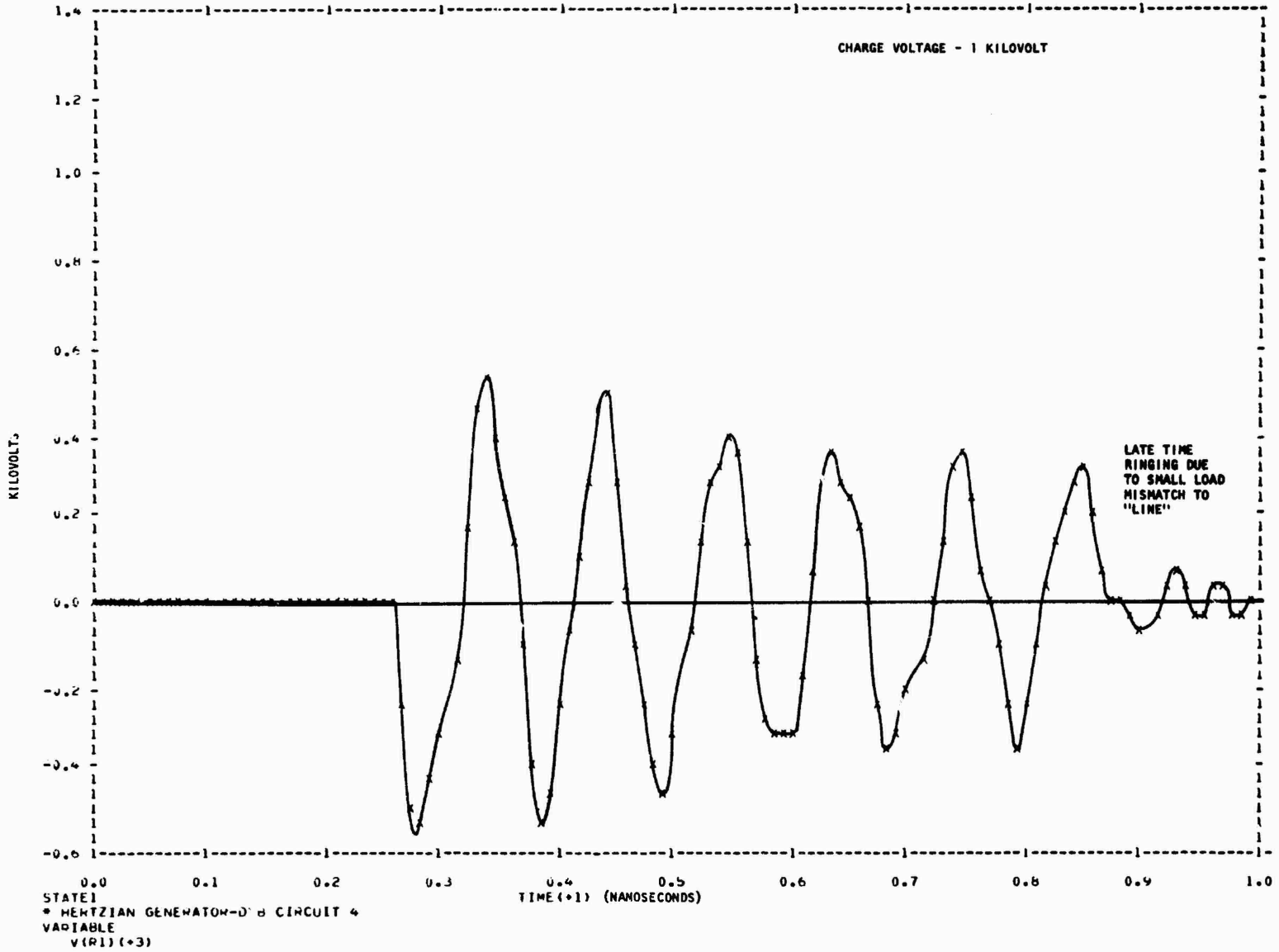

Figure 11. Six-Segment FWG, 1.2 Ohms Per Gap

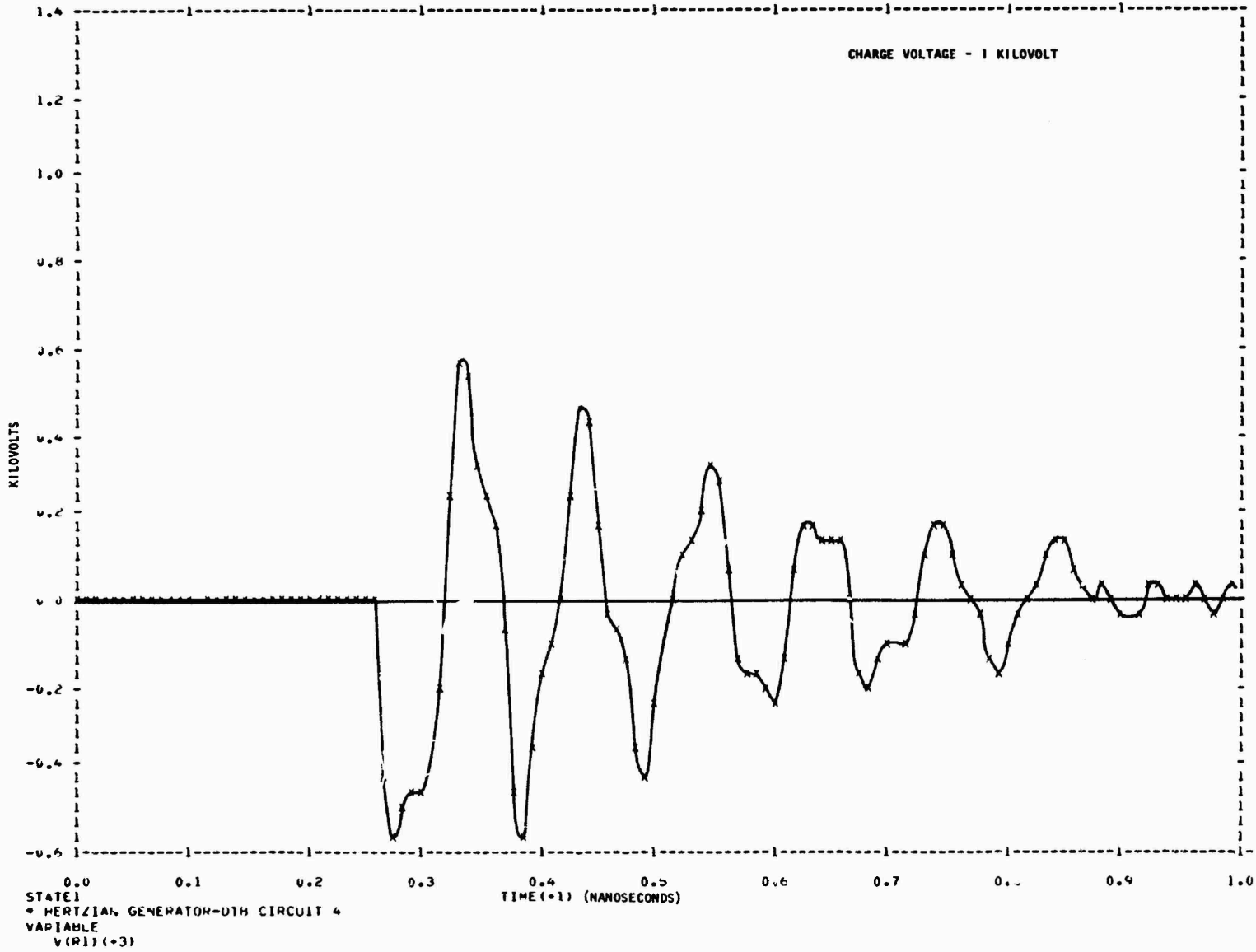

Figure 12. Six-Segment FWG, 3.0 Ohms Per Gap

5. CRITICAL EXAMINATION OF DATA AND THEORY

The experimental data, both from our effort and other investigators, were given a closer examination as well as all of the available theoretical literature. Most of the other experimental data were not directly applicable to our desired results and so could not be used as an absolute verification of the validity of extrapolations of various theoretical formulations.

Several questions had been raised up to this point. One had to do with the length of time required to change a discharge from an ionizing, low current to a low resistance, high current plasma. Historically, this has been a "fast process" given as being somewhat faster than the resolution capability of the investigator's instrumentation and has progressed from a few milliseconds to a subnanosecond event. The present desired application, however, needed at most a few hundred picoseconds and preferably a few tens of picoseconds for this process. Some of the more recent papers contained suggestions that the formative risetime might be a limiting phenomenon.

A second question was that of the minimum obtainable formative delay time jitter of the gap ionization process. If one does indeed find that the periodicity of formative delay times reported by Nesterikhin is general and valid, the effort to reduce the delay to a minimum becomes an effort to produce delays that are all equal. This latter effort may be a less difficult requirement.

The important point appears to be a minimum formative delay or breakdown time ≈200 psec for a system with claimed resolution capabilities of ≈50 psec. The gap materials are not detailed but brass and aluminum are stated to have no effect on these times. The conditions tested were apparently for air at pressures between 160 and 1100 mmHg and for uniform

field electrode at spacings from 0.62 to 1.22 mm. An 18 kV pulse was used for overvoltage factors between 2.8 and 4.5.

Reexamination of various data from other authors also suggests that there may be periodicity of quantization of breakdown times for a wide range of conditions. However, most data presented are apparently near the limit of time resolution for the various author's instrumentation. It is also possible that there is a certain amount of physiological effect in reading the original data which were usually oscilloscope trace photos. So far as is known now, no other authors before have commented on this quantization effect and thus, their data have not been specifically organized or examined to show this.

There are possibly two methods to overcome this jitter limitation [illegible] high frequency frozen wave operation. The first is to use the shortest [illegible]sible gap spacing (i.e., one less than 0.1 mm). The second method is to use some scheme to introduce a sufficiently large number of free electrons into the spark gap working volume to insure breakdown in exactly one avalanche cycle. This might be achieved by use of high intensity light sources, high working voltages for field emission, low work function contaminants in the electrode material, or pulsed x-rays perhaps.

The third question was to examine the various probable energy loss mechanisms of the arc formation. It has been fairly well established that the dynamic resistance of high current arcs that have been established for a few μsec is on the order of, or less than, 1 Ω for atmospheric gas pressure. Additionally, metal vapor arcs at currents ≈Kamps have dynamic resistances of about 5 mΩ but for all these cases there is a fixed, nonzero arc voltage for extrapolated values of low current (15). We have not found much published data concerning the measured resistance of arcs a few hundreds of picoseconds to a few nanoseconds after formation and/or

confined by a few atmospheres pressure of an insulating gas. The literature does suggest that arc resistance decreases with decreasing confining pressure, increasing current density, and increasing time since initiation. This leaves the possibility of a lossy resistive component in arc behavior in the region of time, pressure, and current of interest to this project. If a crude model of a frozen wave generator is taken as a series of n transmission line segments of Zo characteristic impedance with the inner conductors coupled through series resistors $\left(R_{arc}\right)$, one can expect significant losses as n increases or R_{arc}/Z_o departs appreciably from zero.

a. Conclusions Regarding Frozen Wave Generator Operation

Considering what data are available, the certainty of multiple spark gap operation at rise and jitter times of less than 100 psec is low. This would suggest that it may not be practical to operate a pulse device at much above 1 GHz even with carefully optimized materials and circuitry.

The available risetime and jitter with atmospheric gaps suggests an upper frequency limit of about 100 MHz with pulse amplitudes of about 5 kV. Operation under such circumstances would be with a small number of gaps (≈10 or less) with an improved triggering method.

A 370 MHz Landecker pulser has been built with little apparent difficulty (and several pulse generators near 100 MHz also) by use of pressurized spark gaps. That work was done by Dolphin and Wickersham at SRI in 1965 (5).

It is possible that slight modifications of the frozen wave operation could be achieved above 1 GHz, perhaps by the use of closely coupled cavities excited by spark sources. See, for example, Voltaggio and Pinkowski article in Microwaves magazine, May 1973.

b. General Spark Gap Operation

Some of the available literature has been examined to seek both confirmation of the present resuits, and to make estimates of the direction and extent of improved operation available. Conflicting or uncertain results do not seem too uncommon an occurrence. Apparently, the problems of accurate signal sampling or attenuation and adequate waveshape resolution are widespread.

Other workers have deduced that the formative or breakdown delay is statistical in nature and controlled mostly by the electrode material and surface condition. The rate of closure or formative risetime once some current begins to flow is also statistical in nature but largely independent of the initial delay. This last is controlled by the local field strength and the insulating gas condition. All this is fairly well known and in principal, one could select the conditions required for any breakdown delay and formative risetime desired.

c. Pressurized Gap Operation

In order to obtain the desired risetimes both short gap spacings and high overvoltages must be achieved. It is now apparent that this will require a pressurized gaseous or liquid dielectric in the spark gaps proper and probably for the total system. If a dry nitrogen environment is to be used the minimum pressure for the desired output power is on the order of 10-50 atmospheres. This, of course, complicates the mechanical and optical considerations of any system design. The use of liquid dielectrics (e.g., fluorocarbon compounds or deionized water) is attractive from a standpoint of the confining pressure required but the possibility of component damage due to hydraulic shocks generated in the liquid should be considered. Shock damage in a high pressure gas system could also be significant. Insulator properties and insulator conductor interface properties begin to show very strong dependence upon surface conditions with increasing pressure.

Some of the insulating plastics (e.g., methyacrylate types in nitrogen), show an approximately uniform surface flashover insulating strength independent of spacing between electrodes above a critical pressure of about 500 lbs/sq. in. This is for the case of slow double exponential pulses (1 x 50 psec) up to an electrode spacing of about 1 inch. Not all dielectrics behave in this manner. (11)

At the increasingly higher voltage gradients potentially available with pressurized systems special care must be taken with all "triple points" (i.e., the region where solid dielectrics, gas dielectrics, and conductors meet) in order to avoid corona problems. This will increase the mechanical complexity and reduce the allowable dimensional tolerances of the overall system.

d. Controlled Atmospheric Composition

The desired pulse rate of operation, (on the order of 400 pps) combined with the output power desired, will place some important limits on arc quenching times. Residual ionized molecules or excited atoms must be rapidly removed from the neighborhood of the spark gaps. This strongly supports the exclusion of all free oxygen gas and the use of light complex molecules that can remove excitation energy by thermal means. Hydrogen - Helium mixtures can achieve at least part of this requirement and a flowing gas system to physically flush the neighboring volume is also worth considering. A gas velocity of about 100 meters/second in the vicinity of the spark gap can clear, for example, a 5 mm path length in about 50 μsec. Of course, increased gas pressure will also speed the quenching mechanism.

An additional need for control of the environmental gas composition is the operating voltage requirement. An electronegative gas is useful to improve the holdoff time of any given gap geometry and voltage. The most economical, at least from a laboratory experimental viewpoint, is a 10 or 20 percent SF_6 in dry N_2 mixture. A 20 percent

SF_6 mixture has approximately 2-1/2 times the breakdown strength that Nitrogen does under the same pressure and gap geometry conditions. This will reduce the pressure confinement requirements somewhat.

CO_2 is also a potentially useful additive to an insulating gas system. Mixtures of CO_2, N_2, and SF_6 can be used to achieve insulating strengths about equal to high SF_6 ratio mixtures and would decrease the use of this expensive gas. (11) This is probably offset by the lack of commercial availability of the desired mixtures with consequent expense and equipment required for multicomponent gas metering and mixing in the laboratory.

A disadvantage of complex or potentially decomposible gas mixtures is the requirement to maintain component composition within some limits and to remove decomposition products formed during the life of a gas filling. In a laboratory environment, a requirement for frequent flushing and refilling may be tolerable. One would expect, however, that a field usable piece of equipment should be totally self-contained with no maintenance or adjustment required during the course of any mission life. Additionally, even if the decomposition products have a strong tendency to reunite such products are potential corrosives of the electrode materials. It is known, for example, that brass electrodes discolor and erode rapidly in SF_6 environments.

e. Gap Geometry and Material Considerations

Over the range of conditions measured here the pulse formative or apparent risetimes seem to be very nearly proportional to the gap length for any given material geometry conditions. No specific data have been collected to detail this relationship but for brass electrodes in air a risetime of 2-1/2 to 3 nsec was easily obtained for gaps of 1.5-1.7 mm while 1 nsec risetime was not obtained with gaps any wider than .38 mm. One might expect this to yield the desired risetimes

(for high frequency systems) for gaps on the order of or less than .02 mm. The effect of the required gap pressurization upon risetime is not known at this time but may follow an E/P relationship found by others for wider gap spacings. Since dielectric strength does not increase exactly with increased gas pressure the formative time is expected to degrade.

Electrode surfaces of approximately spherical contour, at least in the region of the spark are perhaps the most practical and in view of the probable minimum dimensions of the electrodes the radius of curvature will be large with respect to the gap spacing. This will produce a nearly uniform field condition except that the detailed nature of the surface finish will become quite important at the closer electrode spacings. Exploration of specially shaped electrons may prove beneficial and should not be specifically excluded. The "cookie cutter" electrodes suggested by Proud (15) are indicative of further progress possible.

Optical triggering of increasingly smaller active spark gap volumes become more difficult as they are more nearly shadowed by the local electrode configuration. When the gap spacing is small with respect to the electrode radius of curvature, it is more difficult to adequately illuminate the electrode surfaces at the closest gap spacing and illumination elsewhere will lead to the longer pulse formative times. A longer effective optical f/n system is required to illuminate more deeply into the electrode gap which, in turn, makes the exact position of the illuminating source more critical.

f. UV Triggering

A definite requirement exists for the use of a single, high intensity, stable, pulsed, ionizing illumination source. A high pressure capillary bore arc is probably the best source from an optical standpoint.

These are potentially a little more difficult to ignite than is the case for an atmospheric arc and have service life limitations due to bore material erosion and evaporation.

If an electrode and generator geometry is selected such that the active spark gaps are visible to each other then it is possible that the requirement for a separate illuminating trigger arc can be removed. This would be a desirable system simplification, but could be impractical from a jitter consideration.

The complications arise from the requirement for simultaneous operation of many gaps. This complicates the triggering requirements significantly because simultaneous operation of multi-gap devices decreases very rapidly with increased closure risetime and jitter.

The W/Cu composite electrodes used change surface character from the initial gray polished appearance to a brown matt zone surrounding a highly reflective but roughened copper colored spot where the arc actually forms. This change occurs in a few hundred pulses and remains fairly stable as long as the currents are limited to about 100 amps. At higher arc currents, the electrodes are more roughened and the metallic copper deposit is not seen. So far, no observations have been made in any environment other than air and the effect of surface contour due to higher currents is not known to us at this time.

This composite is noted for its stability of operation which is taken to mean that the work function does not change rapidly for the presence of other compounds on the surface. Its UV triggering sensitivity also may not change very rapidly.

One possibility for usable light source would be the capillary bore arc mentioned previously, operated in a "keep-alive" or dc mode and

pulsed with an appropriate high current pulse for trigger operation. This could reduce at least one of the jitter sources in the overall scheme of operation. Another possibility would be a pulsed UV laser, such as are now available but which do not operate perhaps, at a sufficiently fast pulse risetime. All of these schemes, and even the present one of a centrally located free air arc, would be materially improved by use of focusing lenses to increase the light intensity available on the electrode surface. This again, increases the mechanical complexity of the system.

One further point is to be considered about operation of a spark gap UV source. The excited molecules or ions in the spark will radiate energy of characteristic wavelengths. If the transmission medium also contains those same molecular species the coefficient of absorption may be quite high for those particular transition levels. This may necessitate the use of a second medium for transmission of the UV trigger energy. Quartz fiber light pipes would probably be the best solution.

6. 200 MHz GENERATOR DESIGN

As stated, the present program has resulted in design details for an improved switch and charging system. Design parameters and sketches for a nominal 200 MHz improved Frozen Wave Generator are shown here. This is a completely enclosed gap, coaxial charge line segment unit with capabilities for operating at 100 psi insulating gas pressure.

The system shown can be configured to have a 6 to 12 cycle bipolar pulse train output depending on the number of charge segments connected to the pressure chamber/switch assembly. If the switches (spark gaps) were lossless then the output energy of the device would increase linearly with the number of charged segments. However, for gap resistance that represents a significant fraction of the line impedance, the later pulses in a pulse train would be greatly reduced in power from the earlier pulses for a many gap switch.

There is then a design trade-off between mechanical complexity for numerous cycles in the output pulse train and late time power loss. If power loss is too great then the simpler 6 cycle embodiment would be favored over the 12 cycle embodiment.

The gap configuration shown in Figure 13 permits either self-triggering or externally controlled triggering. The former is preferred initially for simplicity. For repeatability the scheme would be to introduce a small delay in the charge line to one of the frozen wave segments and adjust one of the gaps on that segment to ensure its breaking down first and triggering neighboring gaps in cascade. The physical dimensions of the switch assembly shown in Figure 14 imply a firing window of less than 1 nanosecond for either 7 gap (6 cycle) or 13 gap (12 cycle) operation. This is sufficient for operation up to frequencies on the order of 400 MHz.

Note that the design frequency quoted (200 MHz) is nominal and set by the length of the U-shaped tubes shown in Figure 13; a design frequency in the range 200 to 300 MHz is recommended.

Design Parameters

Output waveform:	6 to 12 cycles @ 200 MHz
Amplitude:	approximately 32 kilovolts peak to peak
Power out:	approximately 10^7 watts into 50Ω
Energy out:	300 to 600 millijoules
Repetition Rate:	1 pulse train per second

Frequency Diversity: Initial design fixed frequency. Later mods could potentially provide continuous frequency coverage over a 4 to 1 spread with an upper limit around 500 MHz.

NOTE: Power out stated for dry N_2 pressurized system. Later changes to insulating gases such as SF_6 provide potential for a factor of 10 increase in power and energy out.

Initial Design Configuration: 200 MHz Pulse Generator

Figure 13 - Simplified sketch showing U-shaped coaxial charge segments connected to pressure chamber/switch assembly.

Figure 14 - Detailed view of pressure chamber and plate showing spark gaps and optical channels between gaps. The overall construction is solid metal with viewing channels milled in. The pressure chamber will be designed to contain 100 to 200 psig.

Figure 15 - Detailed view of individual frozen wave segment showing gap electrode and isolation resistor. The coax tube is Alumispline 50 ohm high temp, low loss line.

Figure 16 - Voltage standoff enhancement versus pressure for Alumispline.

Figure 17 - Schematic diagram of charging system power supply through isolation resistors.

Figure 18 - Detail of energy storage capacitors and coupled slow gaps.

Figure 19 - Detail of peaking gap assembly.

Figure 20 - Simplified exploded view of support and assembly for pulse generator package.

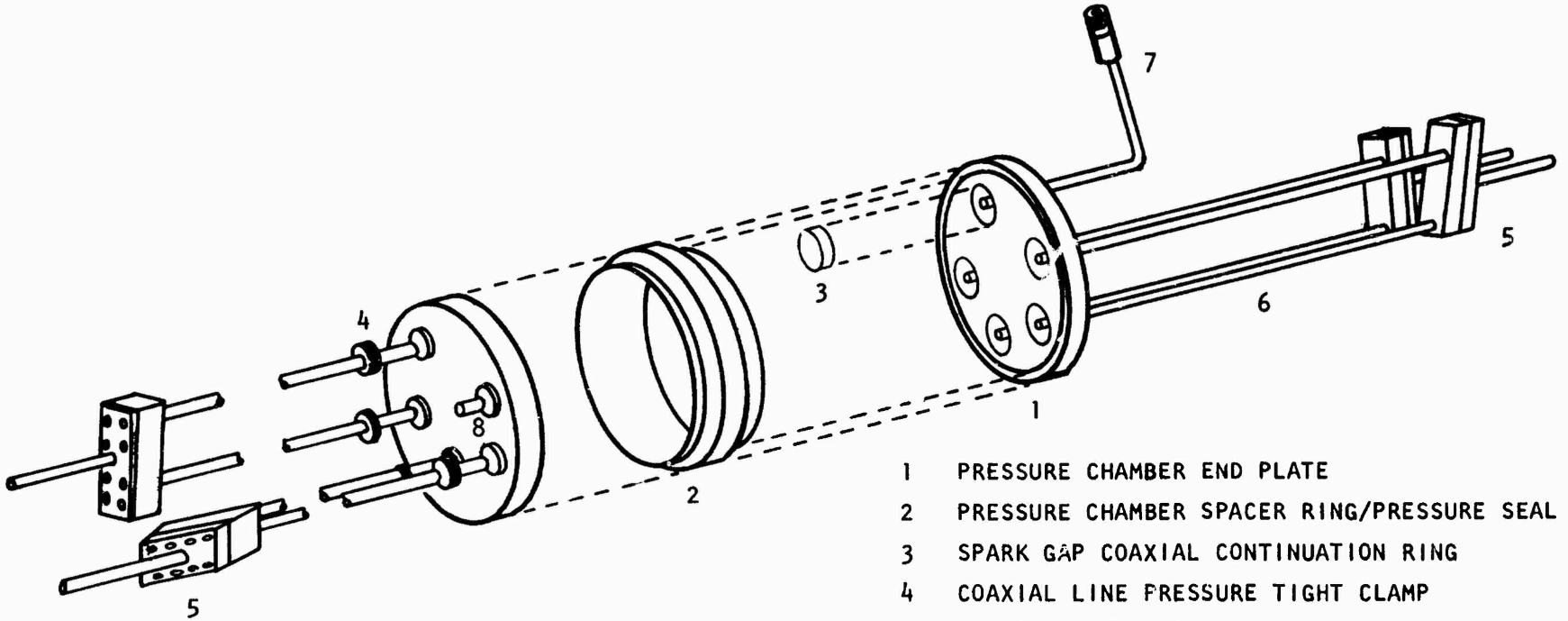

1 PRESSURE CHAMBER END PLATE
2 PRESSURE CHAMBER SPACER RING/PRESSURE SEAL
3 SPARK GAP COAXIAL CONTINUATION RING
4 COAXIAL LINE PRESSURE TIGHT CLAMP
5 COAXIAL LINE CHARGING TERMINAL
6 COAXIAL LINE SEGMENT
7 COAXIAL LINE OUTPUT
8 COAXIAL LINE REFLECTING GAP

Figure 13. U-Shaped Charge Segments Connected to Pressure Chamber/Switch Assembly

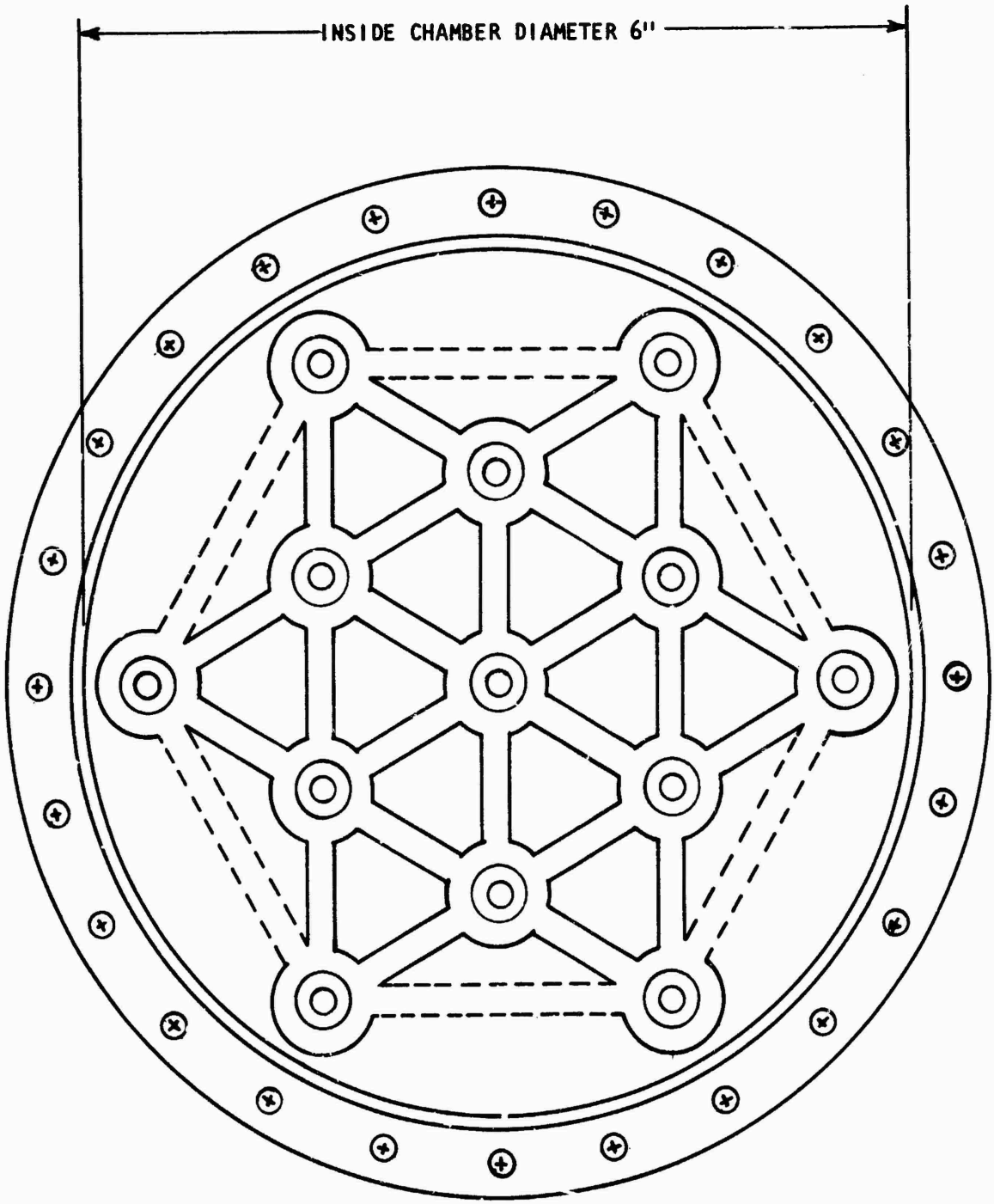

Figure 14. Pressure Chamber and Plate

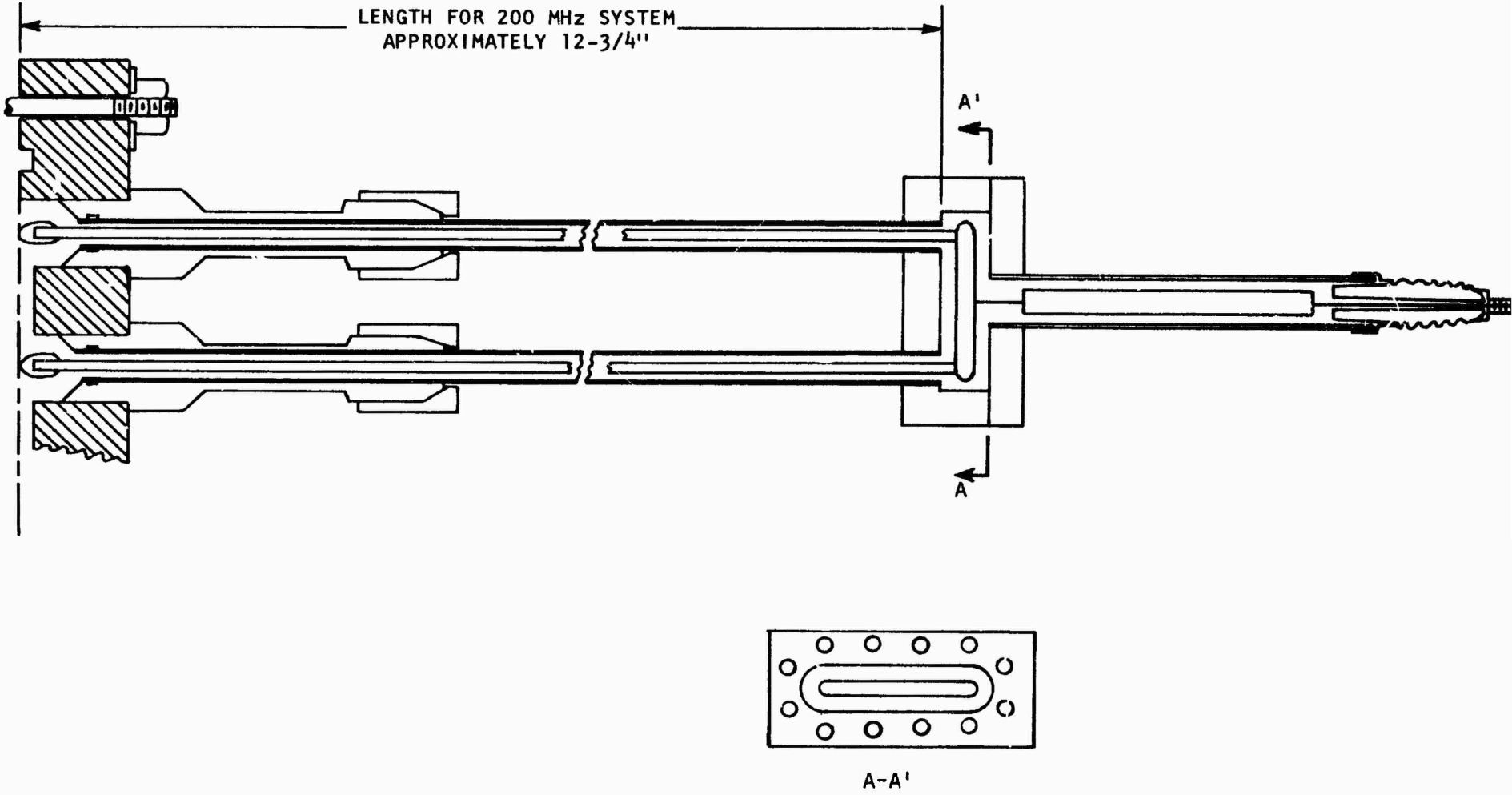

Figure 15. Detailed View of Individual Frozen Wave Segment

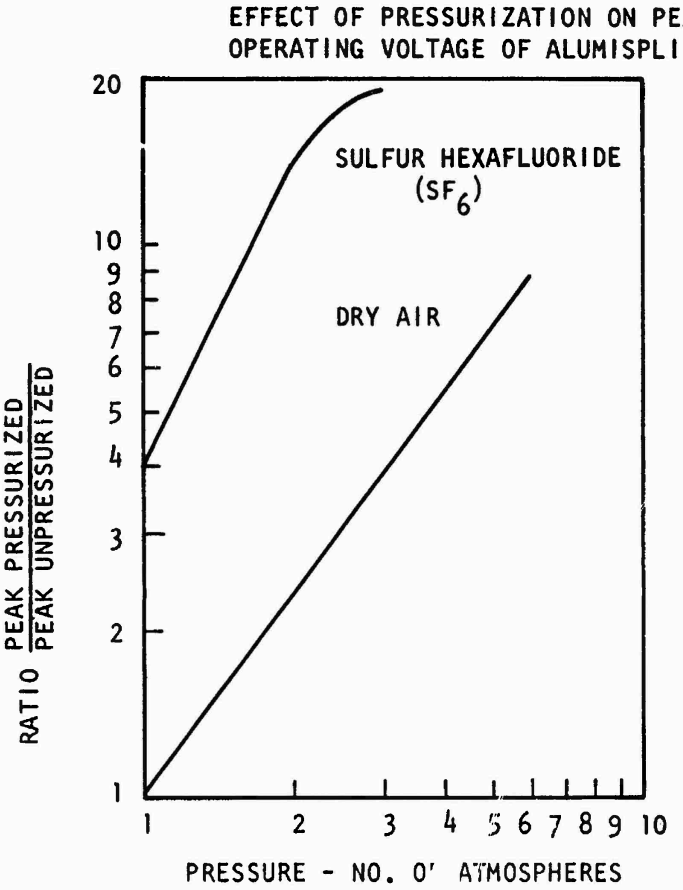

Figure 16. Voltage Standoff Enhancement Versus Pressure for Alumispline

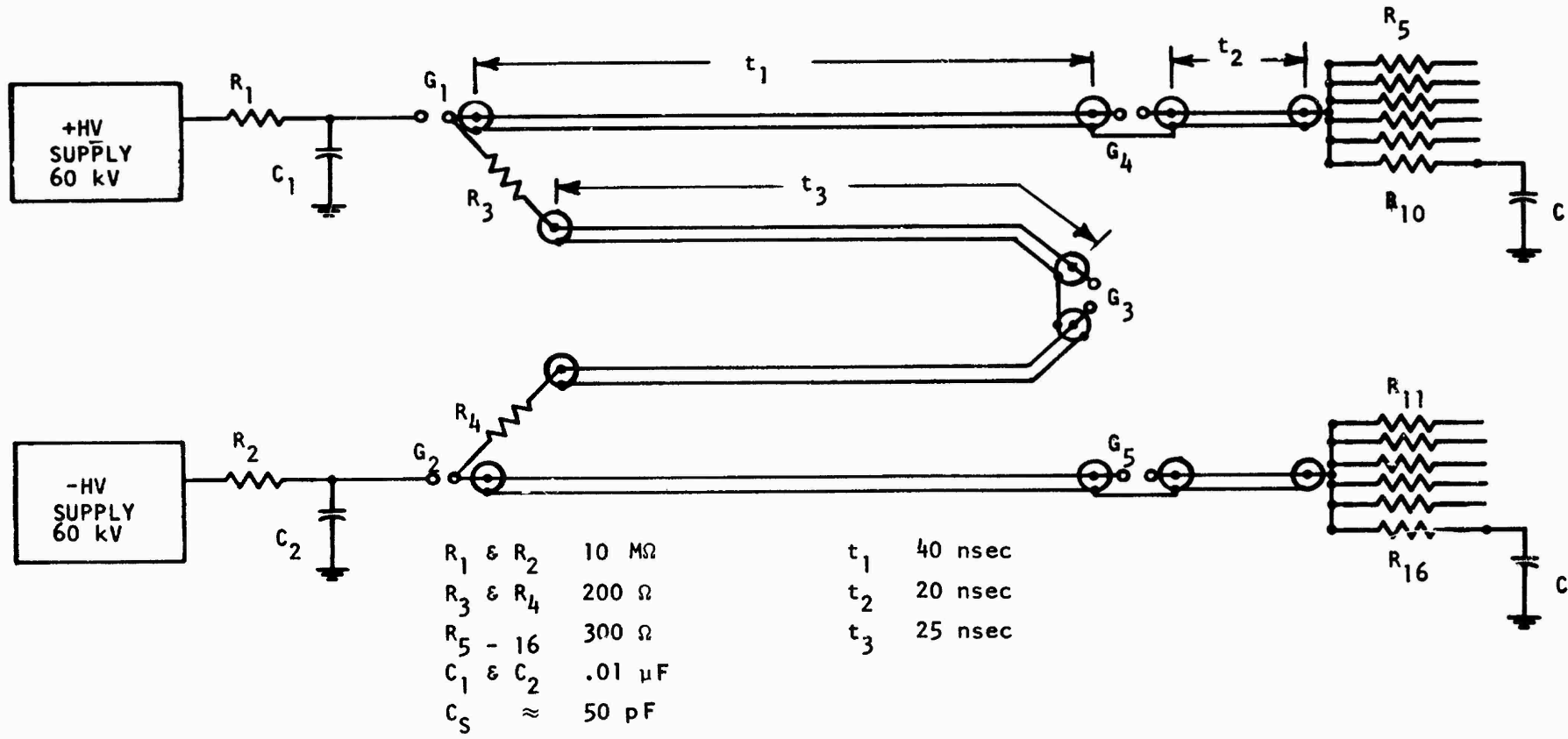

Figure 17. Schematic Diagram of Charging System Power Supply Through Isolation Resistor

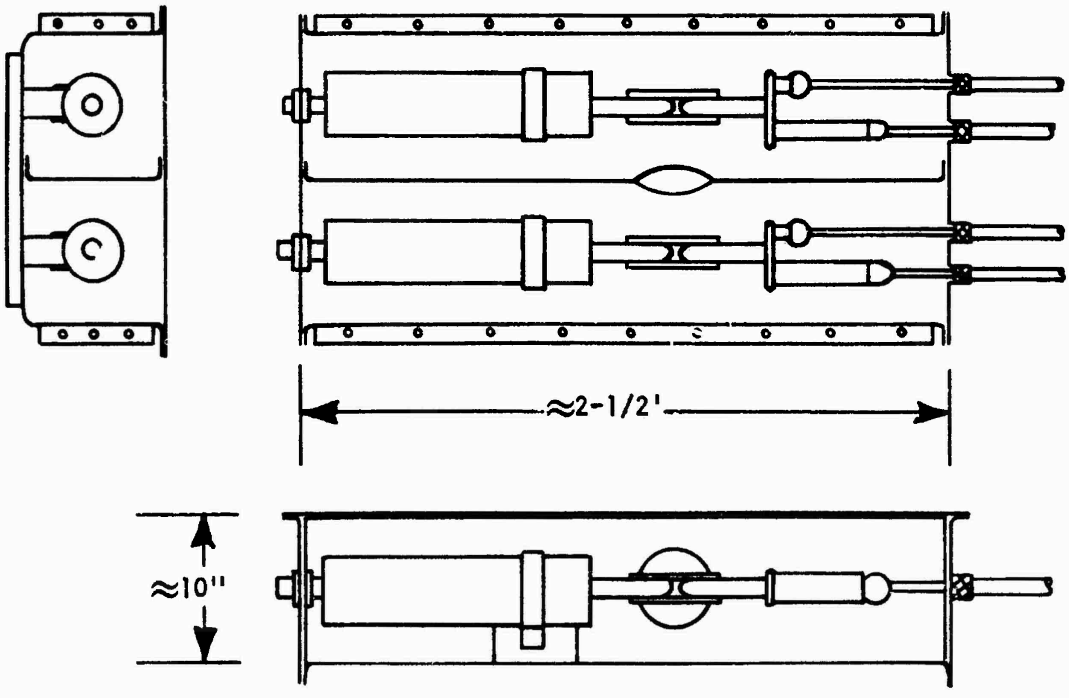

Figure 18. Detail of Energy Storage Capacitors and Coupled Slow Gaps

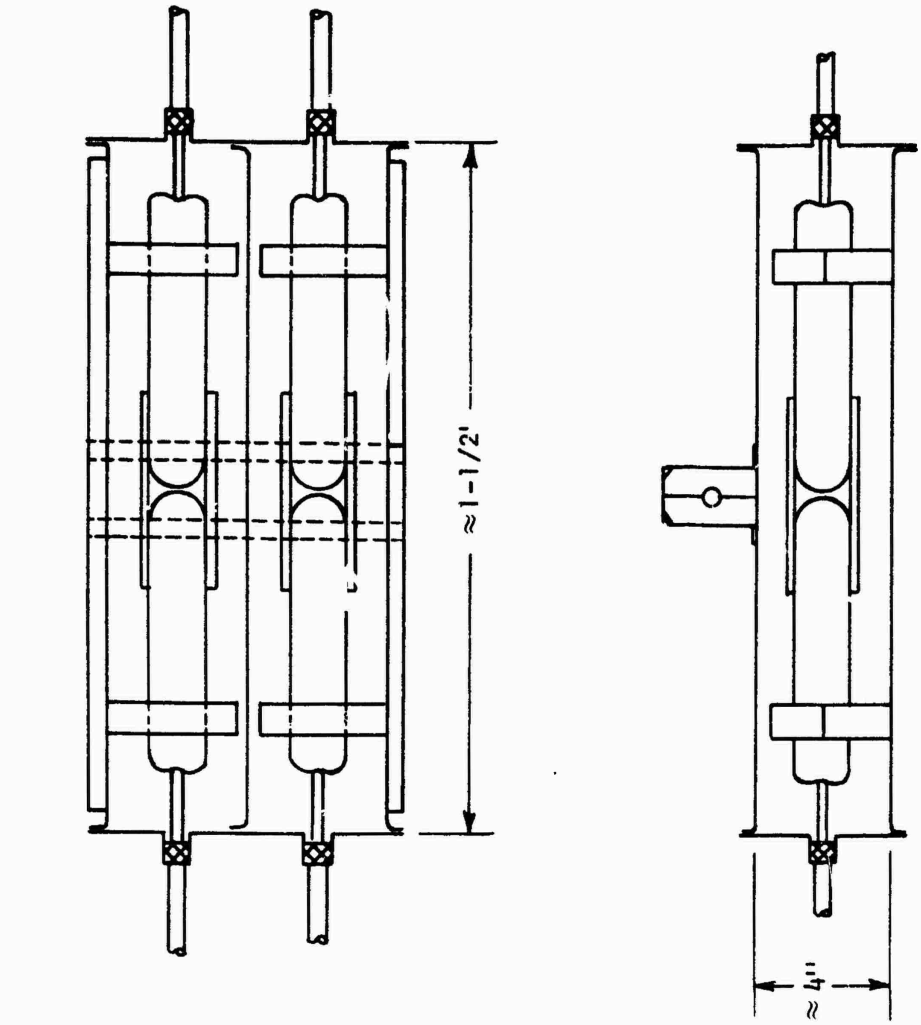

Figure 19. Detail of Peaking Gap Assembly

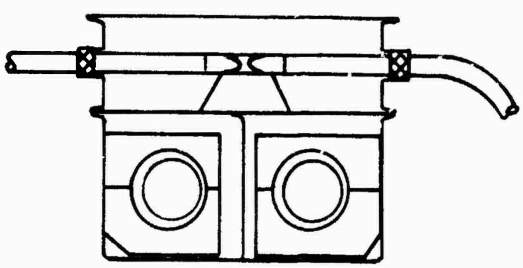

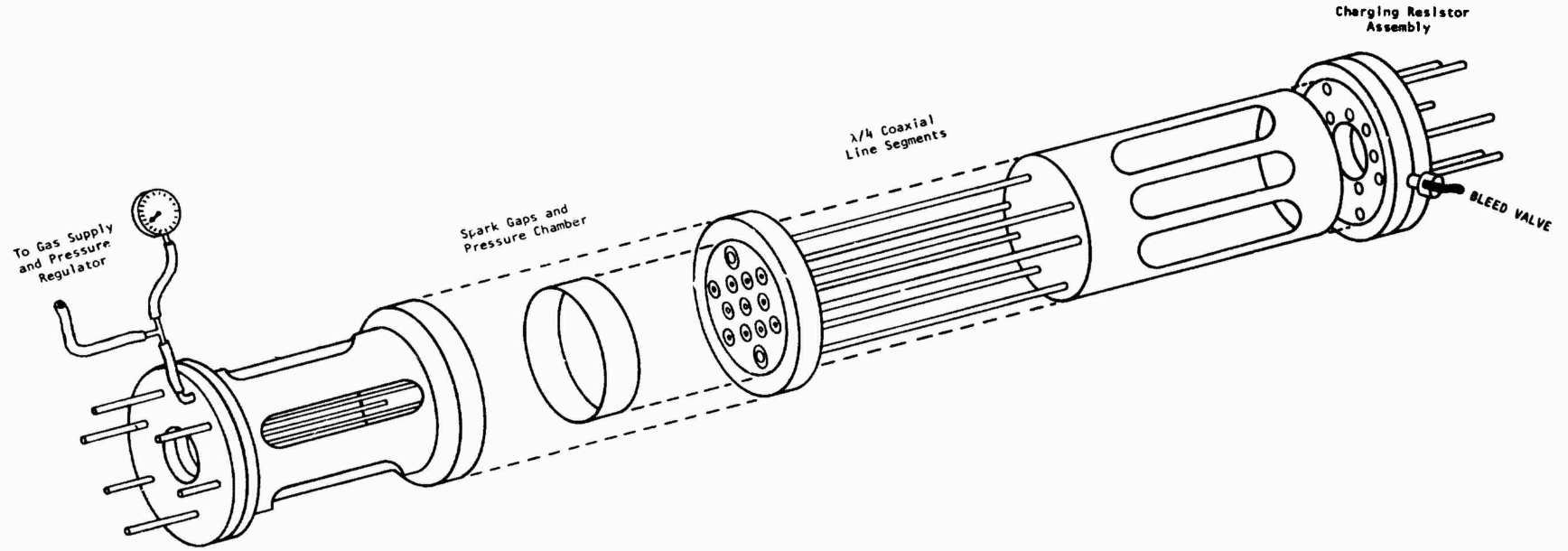

Figure 20. Simplified Exploded View of Support and Assembly for Pulse Generator Package

SECTION V

DESIGN PHILOSOPHY AND GENERAL DISCUSSION

1. GENERAL

In this section the key parameters of achieving suitable spark gap operation are considered. Since this is the most important single feature of a frozen wave pulse generator other parts of such a device are treated as if they were compliant to the requirements of the spark gaps.

Most treatments of gaseous ionization and discharge phenomena find it convenient to treat pairs of variables as a quanity to be determined. Typical of these are E/p, pd, $p\tau$, and $p\Lambda$ where E is the electric field strength, p is the insulating gas pressure, d is the inter-electrode spacing, τ is the formative time, and Λ is a length parameter, usually a diffusion path length. This pairing is useful because for constant values of the paired function a spark gap will behave very much the same even though the individual parameters might be varied over a range of values as much as two or three decades. One must exercise some caution when extrapolating one of the parameters beyond the particular measured range. The most common failure of these paired functions is for very small values of either τ or d.

The sensitivity of the spacing parameter for small values is understandable if one considers the asperities associated with imperfections in surface finish. Further, the closer spacings are more sensitive to the perturbations in local field strength by adjacent conductive and dielectric bodies.

The question of operation at short time intervals is less understood. The best guess at the present time suggests that the process is limited by a combination of avalanche velocity, space charge self-shielding, and recombination and/or relaxation times.

A simplified and rather sketchy understanding of the significance of the paired parameter functions can be had by considering the following. The quanity E/p can be treated as the average voltage across each individual molecule or atom in the dielectric. The outer (or valence) electrons can receive kinetic energy as they move about in the molecule and if the local electric field is strong enough the molecule can be ionized by the stripping of an electron. The quantity pd is a measure of the amount of insulating material in a particular region. This has two obvious functions as pd increases. One is to provide more molecules to absorb the kinetic energy of whatever free electrons are available as long as avalanche generating fields have not been reached. The second function is to provide a greater number of ionized molecules and free electrons per unit volume after avalanche has started.

The quantities $p\tau$ and $p\Lambda$ are only slightly more complex. If one restricts the formative time τ to values sufficiently large that many intermolecular collisions can take place, the average or statistical properties of dielectric molecules can be used rather than the detailed quantum mechanical properties. $p\tau$ then becomes approximately a gross temperature independent term that is a measure of the molecular collision frequency within the insulating medium. Λ is a geometrically determined parameter that is normalized by the voltage applied and the separation distance of the electrodes. Hence, $p\Lambda$ is a normalized form of the term pd that includes the electron mobility.

2. INSULATING GASES

The data presented in Figures 19 and 20 are representative of behavior insulating gases under dc and impulse conditions. The first figure (from Reference 11) gives uniform field data for dc breakdown strength of air as a function of pressure. The test conditions are not certain but the absolute atmospheric pressure was probably near 14-1/2 psi and the gap spacing probably was in the range of 1 to 10 cm for these measurements. At higher pressures the contribution from low work function electrode materials becomes quite important. For lower pressures (150-200 psi) the insulating strength is about linearly proportional to the absolute gas pressure. In the case for pressure considerably below 1 atmosphere and very small gap spacing, a minimum but nonzero breakdown potential is reached which represents an important nonlinearity (the Paschen effect). For our purposes this plot enables one to determine the dc sparkover voltage, given uniform field conditions and gas pressure. Again for our purposes, one may use these data to determine approximate insulating strengths of other gases, given the ratio of breakdown voltage for air and the second gas. This latter process must not be taken to more than 4-10 atmospheres pressure for organic molecular gases as some important nonlinearities occur and electrode material effects can also make significant changes in the curves at higher pressures.

The second Figure, from Reference 6, shows the general behavior of a number of types of gases under impulse conditions. For increasing molecular weight within the same type of gas (monoatomic, diatomic, organic ring, organic chain) these curves shift upward and somewhat to the rignt. The figure is already a plot of three variables for a given gas and is convenient for determining the necessary E/P value to achieve a given spark gap risetime. This plot does not include the statistical delay time to initiate a discharge because the data were obtained with moderate UV illumination of the spark gap. For the case

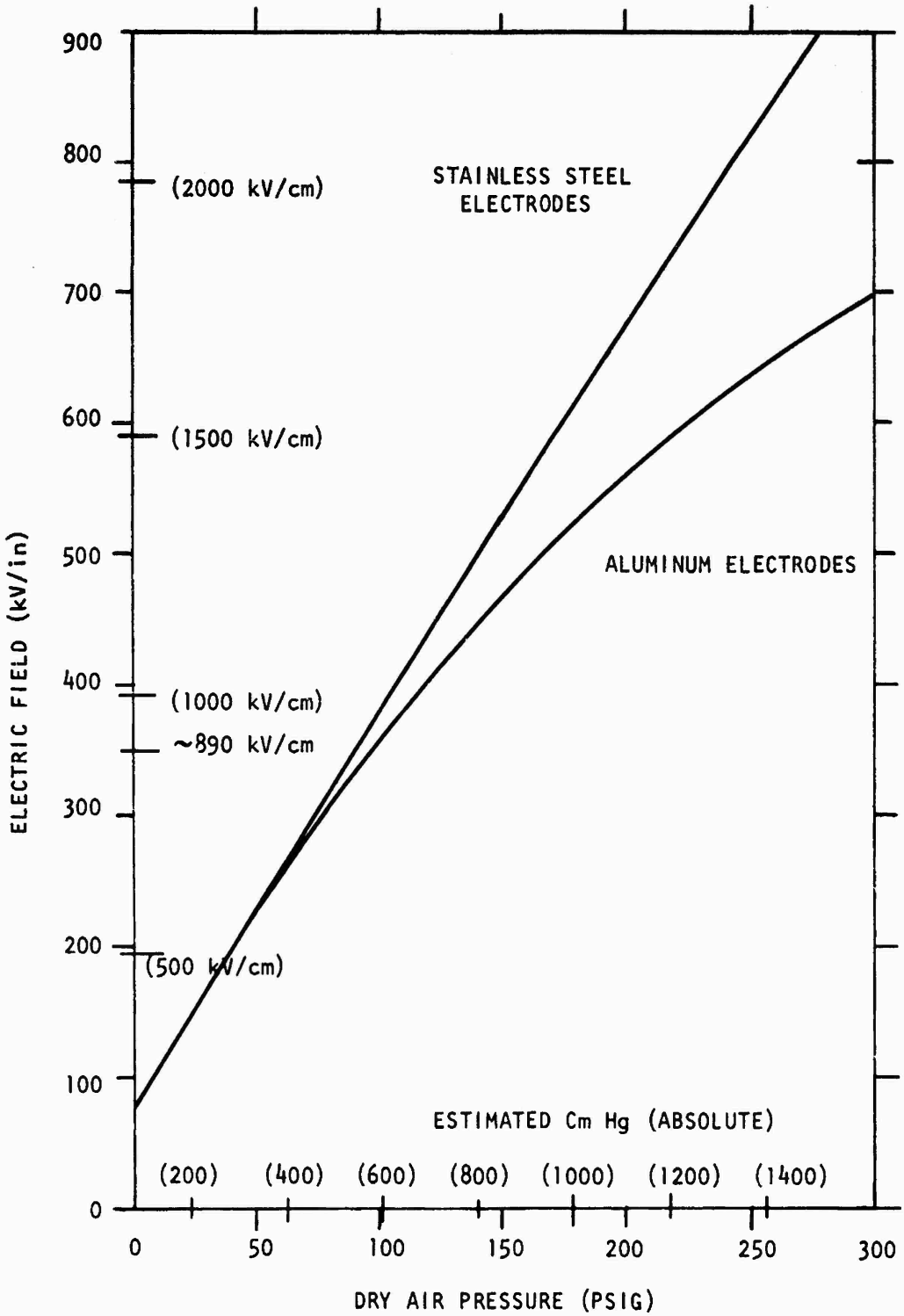

Figure 21. Insulating Strength for Air, Approximately Uniform Field Conditions (Gap Spacing Unknown, From IPC HV Seminar)

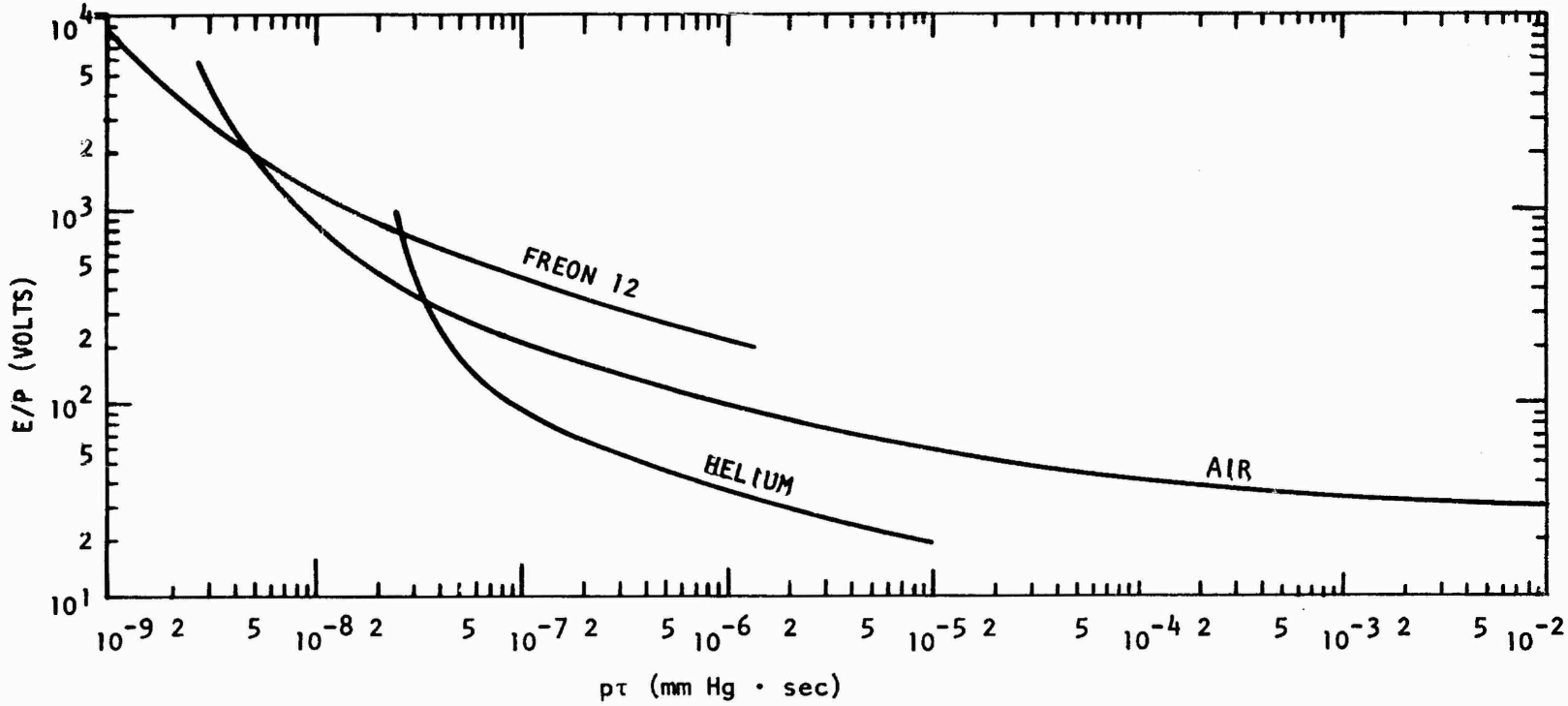

Figure 22. Spark Gap Operation for Uniform Field Conditions for Three Gases

where "fast" operation is required one must use an overvoltage ratio of about 4 or more. This is about the point where one runs into important trade-off for complexity of a pulsed voltage charging circuit.

In estimating the performance of a given spark gap one should note that operating toward the left or upturned end of a curve increases quite rapidly the needed E/P to achieve a given pulse risetime. One is further cautioned to note that the data were obtained for gas pressures in the range of 1-760 mmHg and the resulting times were on the order of a few nanoseconds. Extrapolation to very short times and high pressures is uncertain.

Along this last note of inquiry the paper by Gruber (Reference 8) gives data for air at about 40 psig that fits the curves for air in Figure 20 fairly closely, except for being displaced upward somewhat.

If one is to get on the order of 10^6 watts peak power from a system with characteristic impedance Zo one needs voltage and current capabilities given by

$$V = (Zo\ 10^6)^{1/2} \text{ and } I = (10^6/Zo)^{1/2}$$

for Zo = 50 ohms; V = 7071 volts and I = 141 Amps. These do not appear to be excessive values for present engineering capabilities. Now further, if one wishes a nominal 200 MHz output, the half period time $\tau/2$ will be 2.5 nanoseconds and typical 50Ω coax line would have about 53 pF capacitance for a suitable half period length. At the voltage given above this becomes a stored charge of 0.37 microcoulombs. The charge on an electron is 1.59×10^{-19} coulombs so one has about 2.34×10^{12} electrons to deliver to the load in 2.5 nanoseconds. The question now becomes one of how much energy must be deposited in the active spark gap volume and electrode surface to assure a plasma with adequate free electron density to conduct the current.

For an approximation assume the electric field strength in the gap is sufficient to move free electrons at a drift velocity of C/1000 or 3×10^7 cm/sec and that the gap length is .05 cm, then an average electron will remain in the gap for about 1.67 nsec. This implies that the electron population in the arc is completely replaced about 1-1/2 times during the course of one $\tau/2$ energy release. The effective electron density will then be about 1.56×10^{12} free electrons in the arc at any one time. In actuality all of the electrons will not contribute to the current transfer but rather, some will combine with the insulating gas to form negatively charged ions of various levels of excitation. Perhaps only about 1/3 of the free electrons actually present will be contributing to current flow processes suggesting the need for about 5×10^{12} free electrons in the plasma at any one time. Now if one can assume that it will take about 15 eV of energy to free one electron from a gas molecule each ionization process will require $15 \times 1.6 \times 10^{-12}$ or

24×10^{-12} ergs per free electron. The total energy required to ionize (release) 5×10^{12} electrons is 120 ergs, and the total energy to do this 1-1/2 times is 180 ergs.

The stored energy of 53 pF charged to 7071 volts is about 13250 ergs or about 1.4 percent of the stored energy is required to form the conductive plasma of the arc. This assumes no work function for removing electrons from the cathode surface which will also contribute to the energy requirement.

The energy requirement simplified is given in ergs by the quantity

$$(\text{Amps}) \times (\text{pulse length}) \times (6.24 \times 10^{18}) \times (1.6 \times 10^{-12}) \times 15 \times (\text{plasma electron efficiency})$$

or $\quad I \cdot \tau \cdot \zeta \cdot 1.5 \times 10^{8}$ ergs approximately.

The next question to be answered is does the self generated magnetic field by the current seriously affect various plasma properties?

The standard long wire formula for magnetic field carrying a current is

$$B = \frac{\mu_o i}{2\pi r}$$ where i is the current and r is the distance from the center of the wire. While the actual field near a current carrying plasma is much more complex, this can be used for a first guess estimate. For the above case in which the radius of the plasm column is about 1/3 the gap length at most, one finds

$$B = \frac{4\pi \times 10^{-7} \times 141}{2\pi \times 1.67 \times 10^{-4}} = .169 \text{ weber/m}^2$$

The magnetic field strength inside can be expected to be less and the fact that this is a short current carrying segment between two larger diameter conductors will also give a considerably lower field.

The cyclotron frequency of a free electron in this field is given by

$$\nu = \frac{qB}{2\pi m}$$

$$\nu = \frac{(1.6 \times 10^{-19})(0.169)}{2\pi\ (9.1 \times 10^{-31}\text{kg})} = 4.7 \times 10^{9}/\text{sec or}$$

a period of .21 nanoseconds/period. In actual fact it is reasonable to assume this is an upper frequency limit and that there will be a broad distribution below this frequency. Absorbtion of RF power is very strong close to the cyclotron frequency but this case should be sufficiently removed to give little difficulty. A similar calculation shows the radius of curvature to be about the same as the gap dimensions, a further indication that little effect will be seen from the magnetic field effects.

The following table indicates the range of values r and ν for free electrons moving at right angles to the magnetic field.

Cyclotron frequency and radius for free electrons at indicated velocities and in indicated magnetic fields are given by:

$$\text{Frequency} = \frac{qB}{2\pi m}$$

$$\text{Radius} = \frac{m \cdot \text{Velocity}}{q\,B}$$

$$\text{Velocity} = \left(\frac{2 \cdot 1.6 \times 10^{-19}\ \text{j/eV} \cdot \text{eV}}{m} \right)^{1/2}$$

B (Webers/m^2) =	.01	.02	.05	.1	.2	.5
Frequency =	280 MHz	560	1.4 GHz	2.8	5.6	14
Kinetic Energy (eV)	Radius					
5	.75 mm	.38	.15	.075	.038	.015
10	1.1	.53	.21	.11	.053	.021
15	1.3	.65	.26	.13	.065	.026
20	1.5	.75	.30	.15	.075	.030
25	1.7	.84	.34	.17	.084	.034
50	2.4	1.2	.48	.24	.12	.048
100	3.4	1.7	.67	.34	.17	.067

For illustrative purposes these same numbers have been calculated taking the proposed 200 MHz generator parameters and are listed here.

For:

Peak power = 2×10^7 watts and $Z_o = 50\Omega$

$V = 31.6$ kV $I = 632$ A

Stored charge = 1.67 μcoulombs/line segment

Electrons to be delivered to the load ≈ 10^{13}/line segment

Probable number of free electrons in gap at a time ≈ 2×10^{13}

Ionizing energy required ≈ 711 ergs

Stored energy in line segment ≈ 6.6×10^4 ergs

Approximate lost energy ≈ 1%

Magnetic field near arc ≈ 0.76 weber/m^2

Cyclotron frequency $\leqslant$21 GHz

Radius of curvature for 15 eV electron ≈ 2×10^{-2} mm

SECTION VI

REFERENCES

Specific References for this Program:

1. Bacchi, H & Pauwels, J. C.; Study of a Very Low Jitter Spark Gap: Application to the Realization of a High-Speed Camera. Proceedings of the 9th International Congress on High-Speed Photography, Aug, 70.

2. Bauder, U.; Radiation from High Pressure Plasmas. Journal of Applied Physics, Vol. 39 #1, pgs. 148-152, Jan 68.

3. Bettis, J. R. & Guenther, A. H.; Sub Nanosecond Jitter Laser Triggered Switching at Moderate Repetition Rates. IEEE Journal of Quantum Electronics, Vol. QE-6, #8, pgs. 483-491, Aug 70.

4. Cross, R. C., et al; Dynamics of Capillary Arcs, Journal of Applied Physics, Vol. 42, #3, pgs. 1221-1224, Mar 71.

5. Dolphin, L. T. Jr. & Wickersham, A. F. Jr; The Generation of Megawatt Peak Powers by Modern Spark-Transmitter Techniques, Final Report. SRI 4548, Feb 66.

6. Felsenthal, P. & Proud, J. M. Nanosecond-Pulse Breakdown in Gases. Physical Review, Vol. 139, #6A, pgs. 1796-1804, 13 Sept 65.

7. Fletcher, R.C., Impulse Breakdown in the 10^{-9} sec. Range of Air at Atmospheric Pressure. Physical Review, Vol. 76, #10, pgs. 1501-1511.

8. Gruber, J. E. & Janes, T. E.; Fast Pulse Breakdown of Non-Uniform Field Pressurized Air Spark Gaps. United Kingdom AEA Research Group, Culham Laboratory Preprint CLM-P 171, Mar 68.

9. Guenther, A. H., et al; Low Jitter Multigap Laser Triggered Switching at 50 pps. IEEE Journal of Quantum Electronics, Vol. QE-6, #8, pgs. 492-495.

10. McIntosh, R. E., & Andrews, R. G. Dispersion of Transient Electromagnetic Signals Propagating Along a Co-Axial Gas Discharge. Journal of Applied Physics, Vol. 42, #5, pgs. 1857-1862, Apr 71.

11. Mulcahy, M. J., Gas Insulation, from High Voltage Technology Seminar, Sept. 69.

12. Nesterikhin, Y. E.; et al, Pulsed Breakdown of Small Gaps in Nanosecond Range. Soviet Physics - Technical Physics V. 19, #7, pgs. 29-39, July 64.

13. Pease, M. C. & Karp, A: Microwave Nanosecond Pulse Generator Study, Interim Report #1 RADC-TR-66-572, Oct 66.

14. _____, Same title, Final Report RADC-TR-67-469, Sept 67.

15. Proud, J. M. & Huber, H. J.; Picosecond Risetime Switch Study, Final Report; RADC-TR-67-400, Aug 67.

16. Rich, J. A., et al; Anode Phenomena in Metal-Vapor Arcs at High Currents, Journal of Applied Physics, Vol. 42, #2, pgs. 587-601, Feb 71.

17. Vannicola, V.; Sulfur Hexafloride in High Power Microwave Systems: RADC-TDR-62-443, Nov 72.

18. Taylor, W. C., et al, Measurement of R. F. Ionization Rates in High Temperature Air; Journal of Applied Physics, Vol. 39 #1, pgs. 191-194, Jun 68.

References of a More General Nature:

Raether, H.; Electron Avalanches and Breakdown in Gases. Butterworths, Washington, D.C., 64

Proceedings of the International Conference on Gas Discharges, Sept. 70 London; IEE London 70

Brown, S. C.; Introduction to Electrical Discharges in Gases. Wiley, N. Y., 66.

Proceedings of the High Voltage Technology Seminar, Sept. 69, Boston, Ion Physics Corporation, Burlington, Mass.